

Population effects on the Red Giant Clump absolute magnitude, and distance determinations to nearby galaxies

Léo Girardi^{1,3} and Maurizio Salaris^{2,3}

¹*Dipartimento di Astronomia, Università di Padova, Vicolo dell'Osservatorio 5, I-35122 Padova, Italy*

²*Astrophysics Research Institute, Liverpool John Moores University, Twelve Quays House, Egerton Wharf, Birkenhead CH41 1LD, UK*

³*Max-Planck-Institut für Astrophysik, Karl-Schwarzschild-Str. 1, D-85741 Garching bei München, Germany*

Accepted 2000 ????. Received 2000, July 19; in original form 2000 ???

ABSTRACT

The red giant clump has been recently argued to be a reliable distance indicator for the galaxies in the Local Group. The accuracy of distance determinations based on this method, however, depends on the possible presence of systematic magnitude differences (ΔM_I^{RC}) between the local clump revealed by the *Hipparcos* colour-magnitude diagram, and the clump stars observed in distant galaxies.

In this paper, we re-address the problem of these systematic ‘population’ effects. First, we present tables with the theoretically-predicted *I*-band clump magnitude as a function of age and metallicity. Simple equations, taken from basic population synthesis theory, are provided for the easy computation of the mean clump magnitude for any given galaxy model. We use our models to explain in some detail what determines the distribution of masses, ages, and metallicities of clump stars in a galaxy. Such an approach has so far been neglected in the analysis of clump data related with distance determinations. We point out that, in galaxies with recent/ongoing star formation (e.g. the disks of spirals), the age distribution of clump stars is strongly biased toward younger ($\sim 1 - 3$ Gyr) ages, and hence toward higher metallicities. Obviously, this does not happen in galaxies with predominantly old stellar populations (e.g. ellipticals and bulges).

We construct detailed models for the clump population in the local (*Hipparcos*) sample, the Bulge, Magellanic Clouds, and Carina dSph galaxy. In all cases, star formation rates and chemical enrichment histories are taken from the literature. The *Hipparcos* model is shown to produce distributions of metallicities, colours, and magnitudes, that are similar to those derived from spectroscopic and *Hipparcos* data. The Bulge, Magellanic Clouds, and Carina dSph models are used to analyse the values of ΔM_I^{RC} for these different stellar systems. We show how the clump–RR Lyrae data from Udalski (1998a) is well reproduced by the models. However, despite the similarity between the models and data, the models indicate that the linear ΔM_I^{RC} versus [Fe/H] relations that have been derived from the same data (Udalski 1998a, 2000; Popowski 2000) are not general. In fact, the distribution of clump stars has several factors hidden in it – e.g. the age-metallicity relation, the rate of past star formation – that cannot be described by such relations.

The model behaviour is also supported by empirical data for open clusters by Sarajedini (1999) and Twarog et al. (1999). We argue that Udalski’s (1998b) data for LMC and SMC star clusters do not allow a good assessment of the age dependence of the clump magnitude. Moreover, we remark that similar analyses of cluster data should better include clump stars with ages $1 - 2$ Gyr, which turn out to be very important in determining the mean clump in galaxies with recent star formation.

Finally, we provide revised clump distances to the Bulge, Magellanic Clouds, and Carina dSph, and further comment on their reliability. The largest ΔM_I^{RC} values are found for the Magellanic Clouds and Carina dSph, which turn out to be located at distance moduli $\sim 0.2 - 0.3$ mag longer than indicated by works which ignore population effects. The Galactic Bulge, instead, may be slightly closer (up to 0.1 mag in distance modulus) than indicated by previous works based on the red clump, the exact result depending on the use of either scaled-solar or α -enhanced stellar models.

Key words: Hertzsprung–Russell (HR) diagram – stars: horizontal branch – stars: luminosity function, mass function – solar neighbourhood – Magellanic Clouds – galaxies: stellar content

arXiv:astro-ph/0007343v2 10 Oct 2000

1 INTRODUCTION

The red giant clump has been recently claimed to provide a very accurate standard candle. Once the mean I -band* magnitude of the red clump, I^{RC} , is measured in a nearby galaxy, its absolute distance modulus $\mu_0 = (m - M)_0$ is easily derived by means of

$$\mu_0 = I^{\text{RC}} - M_I^{\text{RC}} - A_I + \Delta M_I^{\text{RC}}. \quad (1)$$

In this equation, M_I^{RC} is the reference value (zero point) provided by nearby clump stars whose distances are known from *Hipparcos* trigonometric parallaxes, A_I is the interstellar extinction to the red clump population of an external galaxy, and $\Delta M_I^{\text{RC}} = M_I^{\text{RC}}(\text{Hipp}) - M_I^{\text{RC}}(\text{galaxy})$ is the population effect, i.e. the difference of the mean red clump absolute magnitude between the local and external samples of stars.

Determining M_I^{RC} and I^{RC} is, usually, less of a problem. Both in the *Hipparcos* database of nearby stars, and in CMDs covering even a small fraction of a nearby galaxy, one typically finds several hundreds of clump stars, clearly identifiable by their position in the CMD. Then, by performing a non-linear least-square fit of the function

$$N(I) = a + bI + cI^2 + d \exp \left[-\frac{(I^{\text{RC}} - I)^2}{2\sigma_I^2} \right] \quad (2)$$

to the histogram of stars in the clump region per magnitude bin [i.e. the luminosity function $N(I)$], the value of I^{RC} and its associated standard error are easily determined (Stanek & Garnavich 1998). The parameter σ_I gives a good indication of how sharp the luminosity distribution of clump stars is, whereas a , b , c (also derived from the fitting procedure) are constants of less interest.

By applying this procedure to the *Hipparcos* database of nearby stars (closer than, say, 70 pc), M_I^{RC} has been determined with accuracy of hundredths of magnitude (Paczynski & Stanek 1998; Stanek, Zaritsky & Harris 1998). Similar accuracies are obtained for I^{RC} in nearby systems like the Galactic Bulge (Paczynski & Stanek 1998), the Magellanic Clouds (Udalski et al. 1998), and M 31 (Stanek et al. 1998). In all cases, the accuracy is limited mainly by the calibration of the photometry, rather than by number statistics of clump stars.

Therefore, the main concerns in the use of clump stars as standard candles are in the determination of the extinction A_I , and the population effects ΔM_I^{RC} . The Magellanic Clouds provide emblematic examples of the problems associated with both determinations. In fact, the first applications of the red clump method to the LMC have provided extremely short distances (e.g. $\mu_0^{\text{LMC}} = 18.1 - 18.2$ mag; see Udalski et al. 1998 and Stanek et al. 1998) if compared with the values commonly accepted a few years ago ($\mu_0^{\text{LMC}} \simeq 18.5 \pm 0.1$ mag; see Westerlund 1997), and in strong disagreement with the latest values derived from classical methods as the Cepheids P-L relation (e.g. $\mu_0^{\text{LMC}} = 18.7 \pm 0.1$ mag cf. Feast & Catchpole 1997). These ‘short’ LMC distances have been suspected to arise from errors in estimating either A_I , or ΔM_I^{RC} , or both.

With respect to A_I , Romaniello et al. (1999) and Zaritsky (1999) recently claimed that the A_I values used for LMC

clump stars in Stanek et al. (1998) are overestimated by about 0.2 mag, thus resulting in an underestimate of μ_0^{LMC} by the same amount. Both argue to obtain more reliable estimates of A_I , either using high-quality multi-band HST photometry as Romaniello et al. (1999), or determining the reddening directly from red stars (from 5500 to 6500 K) in the observed fields, instead of using mean reddening values (Zaritsky 1999).

In this paper, we address the subtle problem of determining the population effect ΔM_I^{RC} . This factor has been initially neglected (Paczynski & Stanek 1998; Udalski et al. 1998; Stanek et al. 1998), after noticing that I^{RC} is remarkably constant, as a function of the $V-I$ colour, in several stellar systems like the Bulge (Paczynski & Stanek 1998), M 31 (Stanek et al. 1998), LMC and SMC (Udalski et al. 1998; Stanek et al. 1998), especially in the colour range $0.8 < (V-I)_0 < 1.5$ which defines the local clump from *Hipparcos* (Paczynski & Stanek 1998). However, Cole (1998) and Girardi et al. (1998, hereafter GGWS98) called attention to the non-negligible ΔM_I^{RC} values (up to 0.6 mag according to Cole 1998) expected from theoretical models of clump stars, and claimed a red clump distance to the LMC larger by about $\Delta M_I^{\text{RC}}(\text{LMC}) = 0.2 - 0.3$ mag. GGWS98, and later Girardi (1999), provided simulations of the red clump in model galaxies which naturally showed the effect of an almost constant M_I^{RC} with $V-I$, and presented significant ΔM_I^{RC} values at the same time.

In two successive papers, Udalski (1998ab) aimed at empirically determining the dependence of M_I^{RC} on stellar parameters. The result was a very modest dependence on both metallicity and age. Namely, $M_I^{\text{RC}} = (0.09 \pm 0.03) [\text{Fe}/\text{H}] + \text{const.}$, was obtained by comparing red clump and RR Lyrae stars in the Bulge, LMC, SMC, and Carina dSph, and assuming $M_V^{\text{RRLy}} = (0.18 \pm 0.03) [\text{Fe}/\text{H}] + \text{const.}$ (Udalski 1998a). Moreover, by comparing the clump in several LMC and SMC clusters, Udalski (1998b) claimed negligible changes in M_I^{RC} for cluster ages ranging from 2 to 10 Gyr. More recently Udalski (2000) fits a $M_I^{\text{RC}} = (0.13 \pm 0.07) [\text{Fe}/\text{H}] + \text{const.}$ relationship to the nearby clump stars with spectroscopic $[\text{Fe}/\text{H}]$ determinations. All together, these results would imply quite modest ΔM_I^{RC} values (less than 0.1 mag for the LMC), thus still supporting a ‘short distance scale’, as opposed to the ‘long distance scale’ provided by, e.g. Cepheids and RR Lyrae calibrated by subdwarf fitting to globular clusters (see Feast 1999 and Carretta et al. 2000 for recent reviews).

Udalski’s (1998ab, 2000) results have been extensively used in subsequent works regarding the clump method for distance determinations. Zaritsky (1999) and Popowski (2000), for instance, attempted to reduce the errors in the red clump method associated with reddening estimates, but assumed that Udalski’s (1998ab, 2000) conclusions were valid. However, there are some potential drawbacks in Udalski’s analyses that we think should be considered in more detail. These drawbacks, in fact, are among the main points we wish to address in this paper.

A subtle one is that M_I^{RC} is assumed either not to depend on ages (as in Udalski 1998a, 2000), or not to depend on metallicities (as in Udalski 1998b). Thus, the presence of an age-metallicity relation (AMR) in the observational data could be masking a possible dependence of M_I^{RC} on both parameters, provided that this dependence were in the sense

* Throughout this paper we will refer to the Cousins I -band

of producing brighter clumps at both lower metallicities and younger ages. And these are exactly the trends indicated by theoretical models.

We should also mention the particular selection of Magellanic Cloud clusters in Udalski (1998b). They are limited to the 2–10 Gyr age interval, that is not the complete range of possible ages of clump stars. Moreover, quite large ‘distance corrections’ were adopted for some SMC clusters in Udalski (1998b; see comments in Girardi 1999), which could also be the source of systematic errors in his analysis of the M_I^{RC} dependence on age. It is worth noticing that, although Udalski (1998b) finds evidence that the clump fades by 0.3–0.4 mag at later ages, this particular result has been ignored in later works, where the clump is simply assumed not to depend on age. At the same time Twarog et al. (1998) and Sarajedini (1999), using data from open clusters with main-sequence fitting distances, reached conclusions apparently in contradiction with Udalski’s ones, i.e. favouring larger dependences of M_I^{RC} on either age or metallicity.

Another point of perplexity to us, is that Udalski (1998ab, 2000) and later Popowski (2000) decide to express the population dependence of the clump magnitude by means of simple linear relationships between M_I^{RC} and $[\text{Fe}/\text{H}]$, and between M_I^{RC} and age. In our opinion, these choices are not justified. To this respect, we notice that similar relations are largely used in stellar astrophysics; but they are, in most cases, well supported by theory. A classical example of this kind comes from RR Lyrae stars, for which a linear M_V versus $[\text{Fe}/\text{H}]$ relation is well documented and widely accepted. However, we should keep in mind that RR Lyrae are very particular objects, which occupy a quite narrow range in both physical (T_{eff}) and population (age, metallicity) properties. Clump stars, on the contrary, do not have such tight constraints: they are almost ubiquitous, with a very large range of ages, metallicities, and T_{eff} s. Clearly, nature has much more freedom to play with the luminosity of clump stars, than it has with RR Lyrae. Why should we expect both types of stars to behave in a similar way? Then, why should we expect linear relations to hold for the properties of clump stars?

To clarify these points, in the following we explore the several systematic effects on M_I^{RC} indicated by stellar evolutionary models. In Sect. 2, the metallicity and age effects are described with some detail. We present simple formulas for computing the mean clump magnitude in a galaxy, then allowing the readers to determine the appropriate value for the population correction ΔM_I^{RC} for any given history of star formation and chemical enrichment. We then present a careful comparison between models and the local clump from *Hipparcos* (Sect. 3), which is particularly helpful to illustrate the different effects involved in the problem, and to understand Udalski’s (2000) results. The clump behaviour in Galactic, LMC and SMC clusters is briefly commented on in Sect. 4. We proceed by modelling the clump in several nearby galaxies, and comparing the results with the data discussed by Udalski (1998a) and Popowski (2000) (Sect. 5). Overall, we find that *systematic effects (at the level of $\lesssim 0.3$ mag) are not only present in any determination of red clump distances to nearby galaxies, but are also hidden in many of the previous analyses of clump data discussed in this regard*. Our final conclusions regarding the red clump distance scale to nearby galaxies are presented in Sect. 6.

2 THE CLUMP AS A FUNCTION OF AGE AND METALLICITY

As in previous works, we will base the discussion of model behaviour mostly on the Girardi et al. (2000) set of evolutionary tracks and isochrones. These models have been extensively discussed in GGWS98 and Girardi (1999). It is worth remarking that different models in the literature – although presenting systematic luminosity differences for the core helium burning (CHeB) stars that have passed through the helium flash – present similar behaviours for this luminosity as a function of either age or metallicity (Castellani et al. 2000). The model behaviour is also supported by empirical data for clusters (see Sect. 4). Moreover, the formulas provided in this section allow the reader to check our results using any alternative set of stellar models.

2.1 Simple models for the mean clump magnitude

In our previous works (GGWS98 and Girardi 1999) we have discussed the behaviour of the clump as a function of mass, age and metallicity, considering mainly the sequences of zero-age horizontal branch models (ZAHB), i.e. of the stellar configurations at the beginning of quiescent CHeB. This time, however, we prefer to discuss the behaviour of the *mean* clump as a function of age and metallicity.

The properties of the mean clump are defined as follows. For a given isochrone of age and metallicity (t, Z), we perform the following integrals over the isochrone section corresponding only to CHeB stars:

$$\langle M_\lambda(t, Z) \rangle = -2.5 \log \left[\frac{1}{N_{\text{cl}}(t, Z)} \int^{\text{CHeB}} \phi(m_i) 10^{-0.4M_\lambda} dm_i \right] \quad (3)$$

where M_λ is the absolute magnitude in the pass-band λ , m_i is the initial mass of the star at each isochrone point, and $\phi(m_i)$ is the Salpeter IMF (number of stars by initial mass interval $[m_i, m_i + dm_i]$). N_{cl} is the *number of clump stars (at age t) per unit mass of stars initially born*. It is simply given by the integral of the IMF by number, along the CHeB isochrone section, i.e.

$$N_{\text{cl}}(t, Z) = \int^{\text{CHeB}} \phi(m_i) dm_i. \quad (4)$$

In our case, the IMF is normalised such as to produce a single-burst stellar population of total initial mass of $1 M_\odot$ (i.e. $\int m_i \phi(m_i) dm_i = 1 M_\odot$), and a mass-to-light ratio of $M/L_V = 0.2$ at an age of 10^8 yr. The details of this normalisation can be found in Girardi & Bica (1993) and Salasnich et al. (2000). It is worth remarking that none of the results presented in this paper depends on the particular choice of IMF normalisation. However, having an IMF normalised to unit mass turns out to be a convenient choice.

From eq. 3, accurate values for the mean clump colours and magnitudes can be obtained. Table 1 presents the values of $\langle M_I \rangle$, $\langle V-I \rangle = \langle M_V \rangle - \langle M_I \rangle$, and N_{cl} obtained for ages ranging from 0.5 to 12 Gyr, and metallicities from $Z = 0.0004$ to 0.03. More extensive tables, suitable to perform accurate interpolation in the quantities (t, Z), are available in computer-readable form in <http://pleiadi.pd.astro.it>. Part of this information is also illustrated in Fig. 1.

Another useful quantity included in Table 1 is the mean initial mass of clump stars,

Table 1. Mean clump properties, as a function of age and metallicity, from Girardi et al. (2000) isochrones.

t (Gyr)	$Z = 0.0004$				$Z = 0.001$				$Z = 0.004$			
	N_{cl} (10^{-4})	$\langle m_i \rangle$ (M_{\odot})	$\langle M_V \rangle$	$\langle M_I \rangle$	N_{cl} (10^{-4})	$\langle m_i \rangle$ (M_{\odot})	$\langle M_V \rangle$	$\langle M_I \rangle$	N_{cl} (10^{-4})	$\langle m_i \rangle$ (M_{\odot})	$\langle M_V \rangle$	$\langle M_I \rangle$
0.5	26.30	2.358	-1.186	-1.521	25.70	2.415	-1.061	-1.591	31.60	2.560	-0.435	-1.259
0.6	29.40	2.191	-0.929	-1.307	30.60	2.245	-0.737	-1.375	37.00	2.386	-0.118	-0.955
0.7	32.30	2.065	-0.685	-1.149	33.70	2.115	-0.467	-1.166	41.40	2.250	0.114	-0.729
0.8	36.80	1.962	-0.466	-1.020	37.60	2.013	-0.259	-0.988	44.30	2.140	0.285	-0.562
0.9	38.00	1.880	-0.318	-0.933	40.90	1.927	-0.073	-0.822	47.20	2.047	0.417	-0.435
1.0	43.50	1.807	-0.148	-0.809	44.40	1.855	0.074	-0.686	50.10	1.967	0.534	-0.321
1.1	44.30	1.750	-0.099	-0.783	47.00	1.793	0.185	-0.585	52.80	1.897	0.632	-0.227
1.2	41.50	1.699	-0.114	-0.816	48.00	1.739	0.245	-0.532	53.10	1.839	0.679	-0.182
1.3	31.00	1.644	-0.164	-0.892	44.00	1.691	0.187	-0.592	52.20	1.789	0.639	-0.227
1.4	20.70	1.595	-0.121	-0.867	28.00	1.630	0.084	-0.715	51.60	1.744	0.514	-0.361
1.5	19.40	1.559	-0.089	-0.844	23.00	1.588	0.105	-0.696	29.60	1.676	0.422	-0.471
1.6	18.70	1.526	-0.059	-0.821	21.40	1.553	0.115	-0.691	22.50	1.632	0.411	-0.488
1.7	17.80	1.495	-0.037	-0.805	20.10	1.520	0.127	-0.682	19.70	1.597	0.400	-0.503
1.8	16.90	1.466	-0.016	-0.788	19.00	1.491	0.139	-0.673	18.20	1.566	0.388	-0.519
1.9	16.00	1.439	0.008	-0.768	18.00	1.463	0.150	-0.665	16.60	1.538	0.387	-0.524
2.0	15.50	1.414	0.035	-0.744	16.90	1.437	0.167	-0.650	16.20	1.512	0.387	-0.527
2.2	14.80	1.371	0.081	-0.703	16.20	1.392	0.198	-0.622	15.50	1.466	0.390	-0.530
2.4	13.50	1.332	0.121	-0.665	14.90	1.352	0.225	-0.597	14.80	1.425	0.415	-0.508
2.6	13.00	1.298	0.155	-0.633	14.20	1.317	0.251	-0.573	14.10	1.389	0.439	-0.487
2.8	12.50	1.269	0.184	-0.605	13.60	1.287	0.273	-0.552	13.30	1.357	0.454	-0.474
3.0	11.50	1.242	0.207	-0.584	12.20	1.260	0.293	-0.533	12.90	1.328	0.465	-0.465
3.2	11.10	1.218	0.226	-0.567	11.90	1.235	0.307	-0.519	12.50	1.301	0.476	-0.457
3.4	10.70	1.196	0.243	-0.550	11.50	1.213	0.321	-0.506	11.80	1.278	0.484	-0.450
3.6	10.30	1.176	0.259	-0.536	11.10	1.192	0.333	-0.494	11.50	1.256	0.496	-0.438
3.8	9.65	1.157	0.275	-0.520	10.50	1.173	0.346	-0.482	11.10	1.235	0.508	-0.428
4.0	9.38	1.139	0.292	-0.503	10.30	1.156	0.358	-0.470	10.80	1.216	0.518	-0.417
4.3	8.98	1.115	0.314	-0.480	9.93	1.132	0.376	-0.452	9.55	1.190	0.534	-0.403
4.6	8.58	1.094	0.335	-0.459	9.57	1.109	0.392	-0.436	9.21	1.167	0.546	-0.391
4.9	8.04	1.074	0.354	-0.441	9.17	1.089	0.407	-0.422	8.87	1.146	0.558	-0.380
5.2	7.80	1.056	0.370	-0.423	8.74	1.071	0.421	-0.407	8.54	1.126	0.569	-0.369
5.5	7.55	1.039	0.385	-0.407	8.44	1.054	0.434	-0.393	7.72	1.108	0.580	-0.359
6.0	7.15	1.014	0.409	-0.381	7.94	1.029	0.455	-0.371	7.36	1.082	0.598	-0.340
6.5	6.75	0.991	0.430	-0.358	7.44	1.006	0.474	-0.350	7.01	1.058	0.613	-0.324
7.0	6.46	0.971	0.451	-0.334	6.63	0.985	0.492	-0.329	6.65	1.037	0.628	-0.308
7.5	6.22	0.952	0.471	-0.309	6.36	0.966	0.509	-0.309	6.23	1.018	0.643	-0.292
8.0	5.97	0.935	0.490	-0.286	6.08	0.949	0.526	-0.289	5.99	1.000	0.657	-0.276
9.0	5.49	0.905	0.524	-0.245	5.55	0.919	0.555	-0.254	5.52	0.969	0.682	-0.246
10.0	4.85	0.880	0.549	-0.202	5.06	0.893	0.585	-0.215	5.14	0.942	0.704	-0.219
11.0	4.71	0.857	0.574	-0.159	4.80	0.870	0.612	-0.177	4.91	0.919	0.723	-0.191
12.0	4.56	0.837	0.595	-0.122	4.55	0.850	0.638	-0.143	4.69	0.897	0.742	-0.164

$$\langle m_i(t, Z) \rangle = \frac{1}{N_{\text{cl}}(t, Z)} \int^{\text{CHeB}} m_i \phi(m_i) dm_i. \quad (5)$$

Figure 2 presents the I -band luminosity function (LF) for several single-burst stellar populations, compared to the mean magnitudes calculated according to eq. 3. It is worth noticing that:

(i) Since the range of clump magnitudes at a given (t, Z) is small, it does not really matter whether the $\langle M_{\lambda} \rangle$ integral is performed over luminosities (as in eq. 3) or magnitudes. The resulting $\langle M_{\lambda} \rangle$ values are always accurate to within ~ 0.01 mag. In fact, what limits the accuracy of eq. 3 is, mainly, the coarseness of the library of stellar evolutionary tracks used to construct the isochrones.

(ii) The intrinsic dispersion of clump magnitudes is slightly larger for younger ages and lower metallicities. For

high metallicities and old ages, the LF of clump stars is characterized by a sharp spike that coincides with the ZAHB bin, and a decreasing tail for higher luminosities. Thus, the mean values $\langle M_{\lambda} \rangle$ are always brighter than the maximum of the LF. This offset is of order 0.1 mag, for the several ages and metallicities considered in the figure.

Therefore, reducing the clump of a single generation of stars to a single point of magnitude $\langle M_{\lambda}(t, Z) \rangle$, should be seen as a useful approximation, rather than the detailed behaviour indicated by models.

So far, the equations and data refer to the clump as expected in single-burst stellar populations, i.e. in star clusters of given age and metallicity (t, Z) . In order to compute the mean clump magnitude for a given galaxy model, of total age T , we need to perform the following integral:

Table 1. (continued)

t (Gyr)	$Z = 0.008$				$Z = 0.019$				$Z = 0.03$			
	N_{cl} (10^{-4})	$\langle m_i \rangle$ (M_{\odot})	$\langle M_V \rangle$	$\langle M_I \rangle$	N_{cl} (10^{-4})	$\langle m_i \rangle$ (M_{\odot})	$\langle M_V \rangle$	$\langle M_I \rangle$	N_{cl} (10^{-4})	$\langle m_i \rangle$ (M_{\odot})	$\langle M_V \rangle$	$\langle M_I \rangle$
0.5	34.30	2.670	-0.113	-1.001	30.60	2.819	0.161	-0.827	29.40	2.821	0.231	-0.827
0.6	40.10	2.492	0.174	-0.718	36.10	2.634	0.399	-0.589	33.90	2.643	0.444	-0.612
0.7	44.90	2.352	0.358	-0.538	40.20	2.491	0.578	-0.410	37.30	2.504	0.609	-0.446
0.8	48.50	2.236	0.508	-0.392	43.90	2.374	0.707	-0.283	40.20	2.391	0.735	-0.321
0.9	51.80	2.139	0.627	-0.276	46.50	2.275	0.812	-0.181	42.90	2.292	0.846	-0.212
1.0	54.80	2.056	0.719	-0.188	48.30	2.191	0.897	-0.100	45.40	2.208	0.936	-0.125
1.1	56.70	1.985	0.791	-0.120	49.90	2.118	0.966	-0.035	46.60	2.137	1.003	-0.061
1.2	54.30	1.930	0.770	-0.148	49.40	2.056	1.006	0.001	47.20	2.076	1.051	-0.018
1.3	53.50	1.874	0.674	-0.251	48.40	2.001	0.994	-0.016	47.10	2.021	1.061	-0.014
1.4	27.80	1.788	0.575	-0.371	48.20	1.950	0.927	-0.091	46.40	1.971	1.040	-0.041
1.5	23.20	1.739	0.552	-0.401	28.20	1.872	0.869	-0.168	45.80	1.925	0.956	-0.142
1.6	20.60	1.698	0.548	-0.410	25.10	1.827	0.828	-0.221	31.60	1.862	0.913	-0.205
1.7	18.80	1.662	0.542	-0.421	22.20	1.787	0.814	-0.243	24.30	1.815	0.937	-0.185
1.8	17.10	1.629	0.542	-0.424	19.50	1.750	0.812	-0.250	20.90	1.777	0.940	-0.187
1.9	16.30	1.600	0.541	-0.429	17.40	1.717	0.814	-0.254	18.90	1.743	0.931	-0.203
2.0	15.30	1.574	0.540	-0.433	16.80	1.688	0.810	-0.263	17.40	1.713	0.926	-0.215
2.2	14.10	1.526	0.556	-0.422	15.50	1.635	0.800	-0.285	16.00	1.660	0.915	-0.236
2.4	13.30	1.484	0.573	-0.409	14.70	1.591	0.794	-0.299	14.40	1.614	0.925	-0.233
2.6	12.80	1.447	0.591	-0.393	13.50	1.551	0.806	-0.293	12.90	1.573	0.938	-0.225
2.8	12.30	1.413	0.610	-0.375	12.30	1.515	0.839	-0.263	12.00	1.537	0.947	-0.221
3.0	11.00	1.383	0.619	-0.369	11.00	1.483	0.868	-0.235	11.50	1.505	0.954	-0.218
3.2	10.70	1.357	0.628	-0.363	10.80	1.454	0.877	-0.230	11.00	1.475	0.959	-0.219
3.4	10.50	1.332	0.635	-0.357	10.70	1.427	0.887	-0.225	10.80	1.448	0.970	-0.211
3.6	10.30	1.310	0.643	-0.352	10.20	1.402	0.893	-0.222	10.60	1.423	0.980	-0.204
3.8	10.00	1.289	0.653	-0.343	9.54	1.380	0.908	-0.208	9.99	1.400	0.987	-0.201
4.0	9.67	1.269	0.665	-0.332	9.09	1.359	0.924	-0.194	9.63	1.378	0.998	-0.192
4.3	9.14	1.241	0.681	-0.316	8.42	1.331	0.945	-0.174	9.23	1.349	1.011	-0.182
4.6	8.29	1.216	0.696	-0.303	7.88	1.305	0.958	-0.164	8.83	1.322	1.023	-0.173
4.9	7.93	1.194	0.705	-0.295	7.72	1.281	0.963	-0.161	8.07	1.298	1.037	-0.162
5.2	7.68	1.174	0.714	-0.286	7.56	1.259	0.969	-0.156	7.69	1.276	1.052	-0.148
5.5	7.43	1.155	0.724	-0.277	7.39	1.238	0.977	-0.150	7.31	1.256	1.067	-0.135
6.0	6.47	1.127	0.738	-0.264	6.38	1.207	0.991	-0.137	6.46	1.226	1.088	-0.116
6.5	6.16	1.101	0.756	-0.245	6.04	1.181	1.007	-0.122	6.06	1.199	1.103	-0.103
7.0	5.87	1.080	0.771	-0.230	5.71	1.159	1.022	-0.108	5.82	1.175	1.115	-0.093
7.5	5.59	1.061	0.784	-0.216	5.32	1.138	1.035	-0.094	5.59	1.154	1.126	-0.083
8.0	5.32	1.044	0.795	-0.205	5.12	1.119	1.046	-0.084	5.31	1.134	1.135	-0.077
9.0	5.02	1.013	0.819	-0.179	4.77	1.086	1.065	-0.065	4.98	1.099	1.159	-0.054
10.0	4.71	0.985	0.840	-0.155	4.48	1.056	1.083	-0.048	4.66	1.069	1.181	-0.033
11.0	4.65	0.961	0.859	-0.131	4.31	1.030	1.103	-0.026	4.53	1.043	1.184	-0.034
12.0	4.42	0.939	0.880	-0.102	4.09	1.007	1.122	-0.005	4.42	1.019	1.191	-0.028

$$\langle M_{\lambda}(\text{gal}) \rangle = \frac{1}{N_{\text{cl}}(\text{gal})} \int_{t=0}^T \psi(t) \langle M_{\lambda}(t, Z) \rangle dt, \quad (6)$$

where

$$N_{\text{cl}}(\text{gal}) = \int_{t=0}^T N_{\text{cl}}(t, Z) \psi(t) dt. \quad (7)$$

The function $\psi(t)$ is the star formation rate (SFR, in M_{\odot} by unit time), at a moment t in the past, for the galaxy model considered. Last but not least, also the age-metallicity relation (AMR) $Z(t)$ should be specified. Notice that we average the magnitudes in eq. 6, instead of luminosities as in the previous eq. 3. The reason for this is that, in this way, we get a quantity similar to the I^{RC} derived in empirical works by means of eq. 2.

2.2 Comparison between different methods

From eq. 6, and the numbers tabulated in Table 1, the reader can easily derive the theoretical mean clump magnitudes for any galaxy model, once the SFR $\psi(t)$ and AMR $Z(t)$ are provided. This is a simple and almost direct way of deriving M_I^{RC} from theoretical models. We will refer to it, hereafter, as **method 1**. There are some additional details about this method, which are worth mentioning:

(i) Some interpolation among the age and metallicity values presented in the tables (e.g. Tab. 1) may be required. In this case, our experience is that the most accurate interpolations in metallicity are obtained using $\log Z$ [or $[\text{Fe}/\text{H}] \simeq \log(Z/0.019)$] as the independent variable, instead of Z .

(ii) For galaxy models with ongoing star formation, the

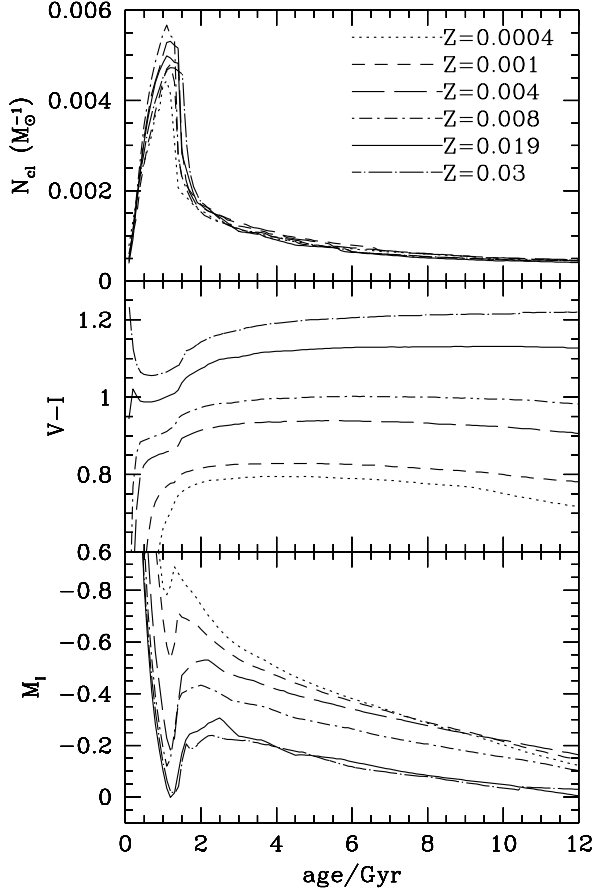


Figure 1. The behaviour of the clump as a function of age, for several metallicities. The top panel shows the current number of clump stars per unit mass of a stellar population, N_{cl} (see eq. 4). The mean $\langle V-I \rangle$ and $\langle M_I \rangle$ (from eq. 3 and Table 1) are shown in the middle and bottom panels, respectively.

integral of eq. 6 should be given a lower-age cut-off of at least 0.5 Gyr. This is because CHeB stars of younger ages, although few, have much higher luminosities, so that they cannot be considered clump stars (see Fig. 1). The final results for M_I^{RC} depend slightly on the choice of this cut-off. In the models discussed in this section, we will assume it equal to 0.5 Gyr.

A second, more refined approach, comes from a complete population synthesis algorithm: synthetic CMDs (or simply the stellar LF) are simulated for a given galaxy model, and then M_I^{RC} is derived by fitting eq. 2 to the synthetic data. This is the approach followed by GGWS98, and will hereafter be referred to as **method 2**. Its advantage is that the synthetic CMDs contain all the information about the distribution of stellar luminosities and colours, which can then be easily compared to actual observations of clump stars. (Additional effects such as sample size, photometric errors, or differential reddening, could also be simulated if required.) However, method 2 is much more demanding, because it requires tools – a population synthesis code, and a non-linear least squares fitting routine – which are not needed in method 1.

For our purposes, the interesting point is to test whether

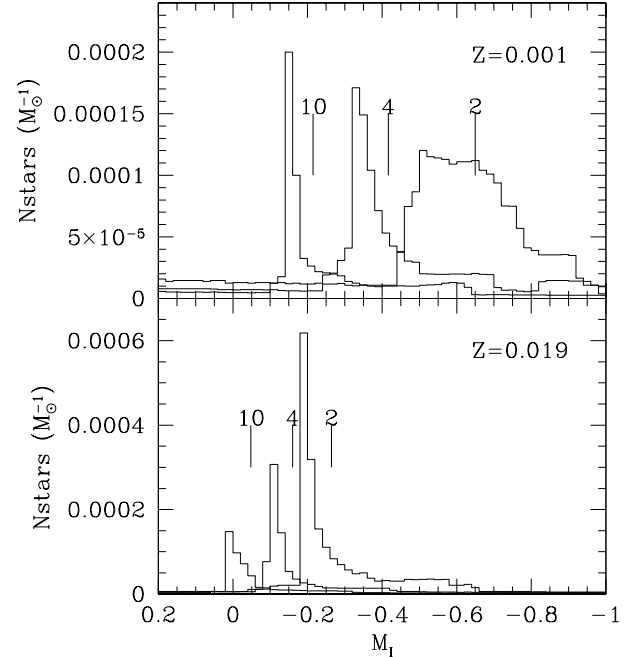


Figure 2. I -band luminosity functions around the clump region, computed with bins 0.02 mag wide, for several single-burst stellar populations. They correspond to isochrones of 2, 4, and 10 Gyr, and metallicities $Z = 0.001$ (top panel) and $Z = 0.019$ (bottom panel). For each isochrone, the mean $\langle M_\lambda \rangle$, as determined from eq. 3, is indicated by a vertical line labelled with the age in Gyr.

Table 2. M_I^{RC} obtained with different methods.

Model	method	M_I^{RC}
Model A	method 1	-0.222
	method 2	-0.187
Model B	method 1	-0.096
	method 2	-0.050

the complexity of method 2 pays for the additional effort with a higher accuracy than method 1. Thus, we verify whether both methods lead to similar results for M_I^{RC} . Using our population synthesis code (Girardi, unpublished), we generate two different galaxy models. The first, **model A**, assumes a constant SFR from $T = 10$ Gyr ago until now, and a metallicity only slightly increasing with the galaxy age $T - t$, i.e. $Z(t) = 0.008 + 0.011 [1 - 0.1t(\text{Gyr})]$. This represents a relatively young and metal-rich galaxy population, as found in the discs of spirals. The second, **model B**, assumes a predominantly old population, i.e. with constant SFR from 8 to 12 Gyr ago, and the complete range of metallicities given by $Z(t) = 0.0004 + 0.0296 [1 - 0.25(t(\text{Gyr}) - 8)]$.

For both models A and B, the mean clump magnitude is computed either with method 1 (table 1 plus eq. 6) or with method 2 (synthetic CMD plus eq. 2). The results are presented in Table 2, and in Fig. 3.

As seen, method 1 provides M_I^{RC} values about 0.05 mag brighter than method 2. This offset results, mainly, from the

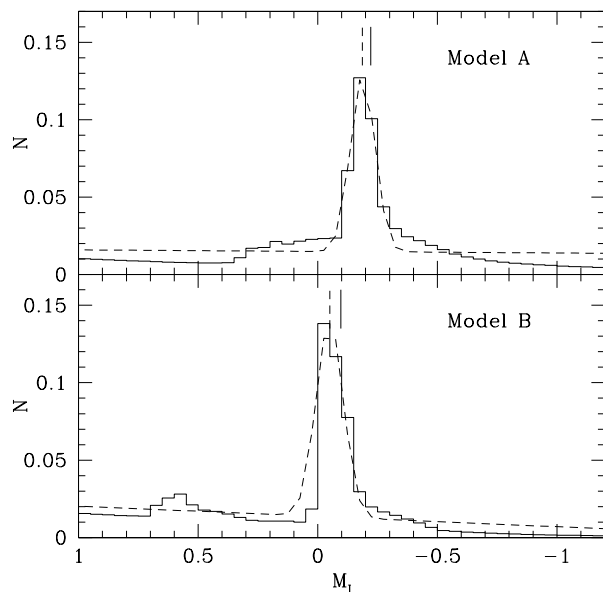


Figure 3. *I*-band luminosity functions for galaxy Models A and B (see text). The continuous histogram represents the synthetic LF as obtained from a population synthesis code, whereas the dashed line is the result of a least-squares fit of eq. 1. For both models vertical lines indicate the mean M_I^{RC} as obtained either with method 1 (continuous) or with method 2 (dashed).

luminosity of the clump LF maximum always being slightly fainter than the mean clump brightness (see Fig. 2): whereas the maximum is more easily accessed by method 2, method 1 always accesses the mean.

Anyway, the important result is that both methods provide almost the same magnitude difference between the two galaxy models, i.e. $\Delta M_I^{\text{RC}}(\text{A} - \text{B})$ is equal to -0.153 cf. Method 1, and -0.137 cf. Method 2 (already on the base of of this simple exercise, we should reasonably expect that the red clump is about $0.14 - 0.15$ mag brighter in a late spiral’s disk than in an old elliptical galaxy). Thus, the results from the two methods turn out to be very similar. In the following we will always apply method 2, based on synthetic CMDs, since it permits to compare in more detail the LF of the synthetic red clump for a given stellar system with the corresponding observational data. Moreover, any value of ΔM_I^{RC} will refer to the difference between the ‘local’ clump simulation and a synthetic model for the stellar system under scrutiny. Our results can be checked by any reader, by using the more simple method 1.

3 AN ANALYSIS OF THE HIPPARCOS CLUMP

The clump stars in the Solar Neighbourhood (or ‘the *Hipparcos* clump’ as hereafter referred) are fundamental for distance determinations based on clump stars, because they provide the only empirical zero point for eq. 1 that can be measured with good accuracy. The ESA (1997) catalog contains ~ 1500 clump stars with parallax error lower than 10 per cent, and hence standard errors in absolute magnitude lower than 0.21 mag. The sample defined by this accuracy

limit is complete up to a distance of about 125 pc. Accurate *BV* photometry is available for these stars (and also *I* for $\sim 1/3$ of them), and the interstellar absorption is small enough to be neglected (Paczynski & Stanek 1998). The Lutz-Kelker bias should not affect their mean absolute magnitude determination by more than 0.03 mag (GGWS98). Therefore, the intrinsic photometric properties of the *Hipparcos* clump can be said to be known with high accuracy, when aspects such as data quality and number statistics are considered.

However, the same can not be said about the population parameters of these stars, i.e. their distributions of masses, ages, and metallicities. Since it was only after *Hipparcos* that a significant number of clump stars was identified in the Solar Neighbourhood (Perryman et al. 1997), few works attempted to describe these stars in terms of their parent populations. This aspect, of course, is of fundamental importance in the present work.

A comprehensive but short discussion of the nearby clump stars’ masses, ages, and metallicities, is presented by Girardi (2000). From this latter work, we select and develop the following points which are more relevant to the present study. More specifically, we discuss general aspects in the mass, age, and CMD distribution of clump stars that may be applied to any galaxy, then focusing on the specific case of the *Hipparcos* clump.

3.1 The mass, age and metallicity distributions: general aspects

The mass distribution of core-helium burning (CHeB) stars in a galaxy of total age T , is roughly proportional to the IMF $\phi(m_i)$, to the core-helium burning lifetime $t_{\text{He}}(m_i)$ of each star, and to the star formation rate (SFR) at the epoch of its birth, $\psi[t(m_i)]$ (where t is the stellar age, and not the galaxy age). There is also a low-mass cut-off, given by the lowest mass to leave the main sequence at ages lower than T . Since $t_{\text{He}}(m_i)$ presents a peak at about $2 M_{\odot}$ (the transition from low to intermediate masses), and the IMF shows a peak at the lowest masses, a *double-peaked mass distribution* turns out for CHeB stars (Girardi 1999). This is shown in the left panel of Fig. 4, for the case of a constant SFR from 0.1 to 10 Gyr ago, and a Salpeter IMF. This distribution contrasts with the more natural idea of a clump mass distribution roughly following the IMF – which would present only a single peak at the lowest possible masses, i.e. at $0.8 - 1.2 M_{\odot}$.

Moreover, from these simple considerations, it turns out that the intermediate-mass stars from say 2 to $2.5 M_{\odot}$, are not severely under-represented in the mass distribution, with respect to the low-mass ones. Stars with $2 - 2.5 M_{\odot}$ are close enough to the clump region in the CMD, to be considered as genuine clump stars (GGWS98). For the case of a constant SFR from now up to ages of 10 Gyr, they would make about 20 per cent of the clump. Again, this contrasts with the common idea that the clump is formed *only* by low-mass stars.

Let us now consider the age distribution expected for clump stars. The number of evolved stars of a certain type and age is proportional to: (1) their birth rate at the present time, and (2) their lifetime at the evolved stage under consideration (see e.g. Tinsley 1980). The birth rate of clump stars, $dN_{\text{cl}}/d\tau_{\text{H}}$, can be estimated as

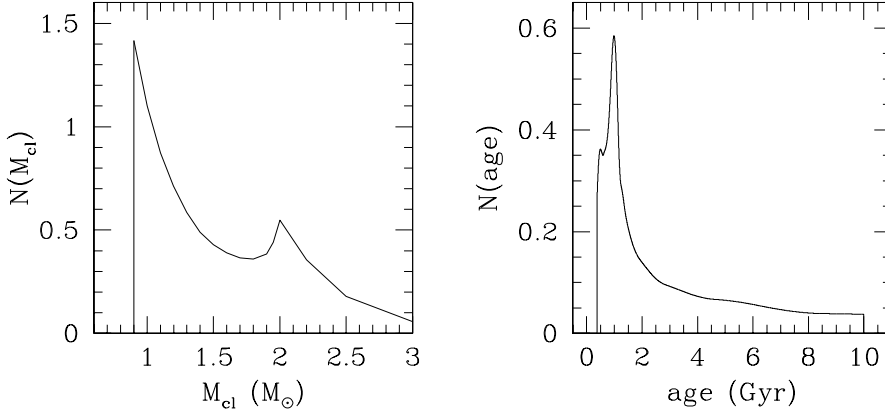


Figure 4. Mass (left panel) and age (right panel) distribution of clump stars for the case of a constant star formation rate (see text).

$$\frac{dN_{\text{cl}}}{d\tau_{\text{H}}} = \psi(t = \tau_{\text{H}}) \phi(m_{\text{TO}}) \left| \frac{dm_{\text{TO}}}{d\tau_{\text{H}}} \right| \quad (8)$$

where m_{TO} is the turn-off mass corresponding to a given main sequence lifetime τ_{H} , and $\psi(t = \tau_{\text{H}})$ is the star formation rate at the epoch of stellar birth.

For clump stars, the age distribution is obtained by multiplying this birth rate by the CHeB lifetime τ_{He} . In the right panel of Fig. 4, we show the result for the case of a galaxy with a constant SFR over all its lifetime. This age distribution turns out to be far from constant: it peaks at an age of 1 Gyr, and decreases monotonically afterwards. In the particular case here illustrated, half of the clump stars have ages lower than 2 Gyr. This result is in sharp contrast with the common idea that clump stars trace equally well the intermediate-age and old components of a galaxy.

These aspects of the age distribution are so important that it is worth commenting on them in more detail:

(i) The continuous decline in the clump age distribution at ages larger than about 2 Gyr, comes, essentially, from the continuous decrease, with the stellar age, of the birth rate of post-main sequence stars. It can be easily understood as follows: between 0.8 and 2 M_{\odot} , the main sequence lifetime scales approximately as $\tau_{\text{H}} \propto m_{\text{TO}}^{-3.5}$ (cf. Girardi et al. 2000 tables), whereas the lifetime of CHeB stars τ_{He} is roughly constant at about 10^8 yr. Together with a Salpeter IMF ($\propto m_{\text{TO}}^{-2.35}$), this implies that $dN_{\text{cl}}/d\tau_{\text{H}}$ (and also the age distribution function) scales as $\propto t^{-0.6}$ for ages $t \gtrsim 2$ Gyr.

(ii) At ages of about 1 Gyr, τ_{He} has a local maximum (about 2.5×10^8 yr, corresponding to the star with $m_{\text{TO}} = 2 M_{\odot}$), which sensibly increases the amplitude of the age distribution at that age.

(iii) At younger and decreasing ages, τ_{He} decreases slightly faster than the birth rate increase of CHeB stars, then causing a decrease in the age distribution function. Even if the number distribution of CHeB stars does not become negligible as we go to younger ages, the ones with ages lower than 0.5 Gyr can hardly be classified as clump stars, since they become much brighter than the clump. This justifies defining a cut-off in the age distribution function for ages $\tau_{\text{H}} < 0.5$ Gyr.

Finally, it should be noticed that, for the case of a constant SFR, the number of clump stars per unit mass of born stars N_{cl} , as obtained from complete population synthesis models (eq. 4), is simply proportional to the age distribu-

tion function of clump stars we have here obtained from simple considerations about stellar lifetimes and birth rates:

$$N_{\text{cl}} \propto \phi(m_i) \tau_{\text{He}} N_{\text{cl}}/dt,$$

This result is just expected, and can be well appreciated by comparing the right panel of Fig. 4 with the upper panel of Fig. 1. The similarity between these two figures, gives us even more confidence in the numbers derived from eq. 4.

The hypothesis of constant SFR, above illustrated, is just a particular case of a most common one, namely that of *continued SFR for most of a galaxy's history* which in general applies to the disc of spiral and irregular galaxies. When the SFR has not been constant, the age distribution function of clump stars can be simply evaluated by multiplying the SFR, at any given age, by the curves in Fig. 1.

3.2 Simulating the *Hipparcos* clump

After these introductory considerations of general validity, let us consider the specific case of the local *Hipparcos* clump. The local SFR is almost certainly not constant, but there are good indications that it has been *continuous* from today back to at least 9 Gyr ago (e.g. Carraro 2000). This continuity renders the age and mass distribution of clump stars qualitatively similar to the cases illustrated in Fig. 4.

Rocha-Pinto et al. (2000b), from a sample of nearby dwarfs with ages determined from their chromospheric activity, find a SFR history marked by several (and statistically significant) ‘bursts’ up to the oldest ages. This work also indicates a volume-corrected age-distribution function which is higher for the youngest stars, as can be seen in Fig. 5. These properties are also supported by other recent works, based on the analysis of *Hipparcos* CMD. Namely, Bertelli & Nasi (2000) favour increasing rates of star formation in the last few Gyr, whereas Hernandez, Valls-Gabaud & Gilmore (2000b) also find evidences for different bursts in a sample of *Hipparcos* stars limited to ages lower than 3 Gyr.

In the following, we adopt the results from Rocha-Pinto et al.’s (2000ab) data in order to simulate the local CMD. This work covers the complete range of ages we are interested in. Before proceeding, we should remind that that stars born at older ages in the local disc, are now distributed over higher scale heights in relation to the Galactic plane. Therefore, in our simulations of the *Hipparcos* sample, we should use the volume-limited age distribution of unevolved dwarfs

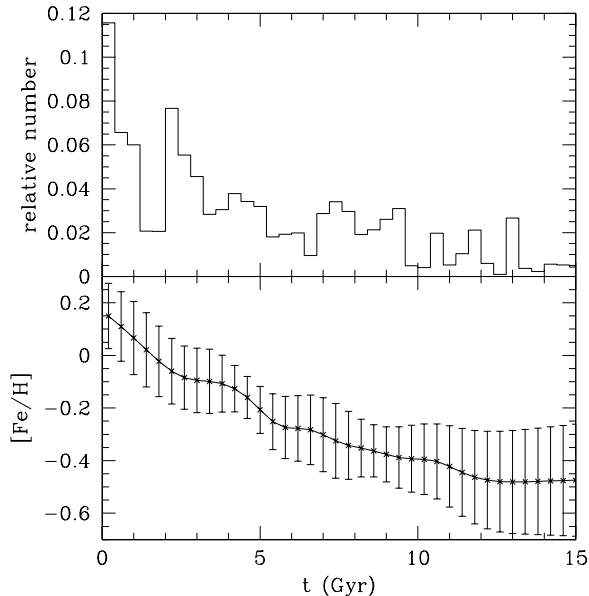


Figure 5. Adopted SFR and AMR for the Solar Neighbourhood. Upper panel: the volume-limited age distribution of local dwarfs as derived from Rocha-Pinto et al. (2000b), sampled at age bins 0.4 Gyr wide. Lower panel: the corresponding values of $[\text{Fe}/\text{H}]$ and its standard dispersion, as derived from interpolation of table 3 in Rocha-Pinto et al. (2000a).

not corrected by any scale-height factor, rather than the cumulative SFR in the so-called ‘solar cylinder’. Rocha-Pinto et al. (2000b) kindly provided us with the uncorrected age distribution we need. Moreover, we have also the possibility of using the local AMR, derived by Rocha-Pinto et al. (2000a) from the same data. Both functions are illustrated in Fig. 5.

Figure 6 shows the final CMD simulated from these data. For the sake of simplicity, we have not simulated – the same applies also to the simulations presented in Sect. 5 – observational errors (as discussed in GGWS98 the inclusion of observational errors increases the width σ_I of the clump stars’ LF, leaving almost unchanged the value of M_I^{RC}). Fig. 7 shows the resulting LF of clump stars from this simulation, together with the result of fitting eq. 1.

Even if in this paper we are discussing population effects (i.e., the value of ΔM_I^{RC} for different stellar systems) on the red clump brightness, and we will use theoretical models only in a differential way, it is nevertheless interesting to note that the absolute value of $M_I^{\text{RC}} = -0.171$ for the local clump as derived from our simulations is satisfactorily close to the observed one, $M_I^{\text{RC}} = -0.23 \pm 0.03$ (Staneek et al. 1998).

3.3 The observed metallicity distribution

Let us now compare the results from our *Hipparcos* simulation, with additional data for nearby clump stars. Their metallicity distribution has been the subject of some unexpected results in the recent past.

There have been few attempts to derive typical metallicities for *Hipparcos* clump stars. The first one has been a quite indirect method by Jimenez et al. (1998). They ap-

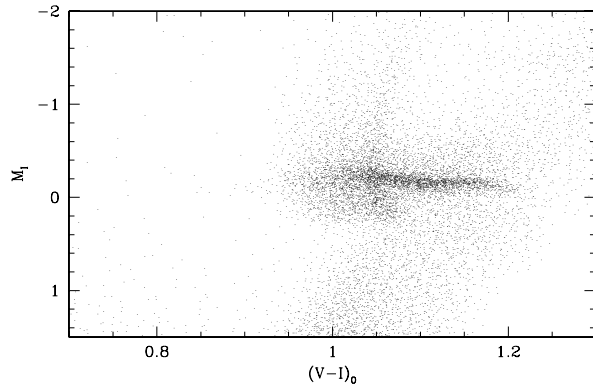


Figure 6. The synthetic CMD, around the clump region, derived from the data of Fig. 5. We assume a total number of 10000 clump stars.

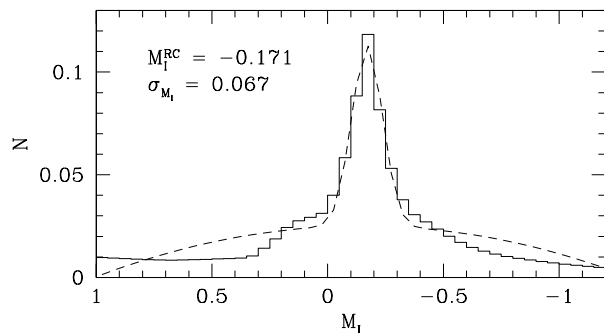


Figure 7. The synthetic LF, around the clump region, derived from the data of Fig. 5. A Gaussian curve (dashed line) has been fitted to the LF with the aid of eq. 1.

plied the concept that red giants become redder at higher metallicities to derive, solely from the colour range of *Hipparcos* clump stars, an estimate of their metallicity range, obtaining $-0.7 < [\text{Fe}/\text{H}] < 0.0$. This approach was based on the fact that in Jimenez et al. (1998) models the clump at a given metallicity is very concentrated on the CMD, and has a mean colour very well correlated with metallicity. In this regard, however, we should consider that the galaxy models considered by Jimenez et al. were characterized by a SFR strongly decreasing with the galaxy age (i.e. increasing with the stellar age). This implies that they were considering, essentially, the behaviour of the *old* clump stars, with masses of about $0.8 - 1.4 M_{\odot}$. Intermediate-mass clump stars with mass $\gtrsim 1.7 M_{\odot}$ were even absent in their simulations. As discussed in the previous Sect. 3.1, this turns out to be an incomplete description of the clump stars, at least in galaxy systems with recent star formation as the Solar Neighbourhood.

In contrast, GGWS98 considered all the interesting mass range of clump stars, and models with constant SFR up to 10 Gyr ago, obtaining clumps with a somewhat more extended distribution in colour than Jimenez et al. (1998). They demonstrate that a galaxy model with mean solar metallicity and a very small metallicity dispersion ($\sigma_{[\text{Fe}/\text{H}]} = 0.1$ dex), shows a clump as wide in colour as the observed

Hipparcos one – i.e. with $\Delta(V-I) \simeq 0.2$ mag. This means that a significant fraction of the colour spread of the local clump could be due to an age spread, rather than to a metallicity spread. Considering the SFR we discussed in the previous subsection, GGWS98 results seem more realistic than Jimenez et al. (1998). It follows that *the colour spread of nearby clump stars cannot be interpreted just as being the result of a metallicity spread* as suggested by Jimenez et al.; the age (mass) spread (from ~ 1 to 10 Gyr) might well be playing an important role.

The above aspect becomes clear when we consider clump metallicities not inferred from broad-band colours. The metallicities of 581 nearby K giants (mainly clump stars) have been derived by Høg & Flynn (1998), based on DDO photometry. From their data it turns out that the $V-I$ colour does not correlate with $[\text{Fe}/\text{H}]$ (cf. Paczyński 1998), contrarily to what would be expected from the Jimenez et al. (1998) analysis.

One may suggest that the problem is in the $[\text{Fe}/\text{H}]$ values inferred from photometry, rather than in the interpretation of clump $V-I$ colours. However, the same problem appears when we look at the most reliable metallicity data, i.e. those derived from spectroscopy. Udalski (2000) selected clump stars with spectroscopic abundance determinations from McWilliam (1990). They mention a non negligible range of clump metallicities ($-0.7 < [\text{Fe}/\text{H}] < 0.0$), and again confirm the lack of $[\text{Fe}/\text{H}]$ versus colour correlation.

We have constructed a similar sample of red giants with spectroscopic abundance determinations. From the *Hipparcos* catalog, we select all red giants (from their position in the colour–absolute magnitude diagram) marked as single stars, with lower than 10 per cent relative error in the parallax, with direct measurements of the $V-I$ colour, and $[\text{Fe}/\text{H}]$ determinations according to the Cayrel de Strobel et al. (1997) catalog. All the $[\text{Fe}/\text{H}]$ values are quoted as being relative to the Sun’s. Nearly half of the selected stars (~ 160 out of 334) are clump stars, the bulk of the remaining ones being in their first-ascent of the red giant branch.

The results can be appreciated in Fig. 8. It presents, in three panels, the quantities M_I , $V-I$, and $[\text{Fe}/\text{H}]$, plotted one against each other. We notice again that, also in this data, $[\text{Fe}/\text{H}]$ and $V-I$ colour seem not to be correlated. A fourth panel of Fig. 8 presents the histogram of $[\text{Fe}/\text{H}]$ values. Interestingly, we find that the $[\text{Fe}/\text{H}]$ distribution of clump stars is fairly well represented by a Gaussian curve of mean $\langle [\text{Fe}/\text{H}] \rangle = -0.12$ dex and standard deviation of $\sigma_{[\text{Fe}/\text{H}]} = 0.18$ dex, as derived by means of a least-squares fit. The surprising feature is *the very small dispersion of metallicities in the data*. It seems to disagree with the wide metallicity ranges mentioned by Jimenez et al. (1998; i.e. $-0.7 \leq [\text{Fe}/\text{H}] \leq 0.0$) and Udalski (2000; i.e. $-0.6 \leq [\text{Fe}/\text{H}] \leq 0.2$). Actually, in the latter case, there is no disagreement at all: the total range of $[\text{Fe}/\text{H}]$ values in our histogram of Fig. 8, is similar to that mentioned by Udalski (2000).

We notice that the small dispersion of clump metallicities, $\sigma_{[\text{Fe}/\text{H}]} = 0.18$ dex, has the same order of magnitude as the one found among coeval Galactic open clusters, after correction for the disc metallicity gradient (figure 4 in Carraro & Chiosi 1994), or among field stars of same age (Rocha-Pinto et al. 2000a; with $\sigma_{[\text{Fe}/\text{H}]} = 0.13$ dex). But how can

we understand such a small metallicity dispersion, coming out for clump stars in a so complex stellar environment as the Solar Neighbourhood? The key to the answer is in our discussion of the age distribution of clump stars in Sect. 3.1: *Actually, nearby clump stars are (in the mean) relatively young objects, reflecting mainly the near-solar metallicities developed in the local disc during the last few Gyr of its history*, rather than its complete chemical evolution history.

It is also interesting to notice that the age distribution of nearby clump stars (mostly K giants), turns out to be very different from that of low-main sequence stars (e.g. the G dwarfs). This because the long-lived G dwarfs have an age distribution simply proportional to the SFR, whereas K giants have it ‘biased’ towards intermediate-ages (1–3 Gyr). This difference reflects into their metallicities: since younger stars are normally more metal rich, giants should necessarily be, in the mean, more metal-rich than G dwarfs. G dwarfs in the Solar Neighbourhood are already known to present a relatively narrow distribution of $[\text{Fe}/\text{H}]$ – the relative lack of low-metallicity stars, with respect to the predictions from simple closed-box models of chemical evolution, being known as the G-dwarf problem. Then, even more narrow should be the distribution of $[\text{Fe}/\text{H}]$ among K giants. And this is, in fact, exactly what is suggested by the observations of Fig. 8.

3.4 The magnitude and colour distribution

In the above subsection, we presented arguments and data which go against the interpretation of clump $V-I$ colours as being mainly due to metallicity differences. This point is also crucial for distance determinations. Were the clump colour determined by metallicity only, the observed constancy of the I -band magnitude with colour inside the clump, in different galaxies, could be indicating that M_I is virtually independent of metallicity, and hence an excellent standard candle (cf. Paczyński & Stanek 1998; Stanek et al. 1998; Udalski 1998a). This latter conclusion comes from a simplified analysis, where the possibility that the clump magnitude and colour depend significantly also on the age, has been neglected.

Let us briefly discuss the specific results we get from our models. In them, M_I^{RC} presents a non negligible dependence on both age and metallicity. Nonetheless, our simulations of the *Hipparcos* clump turn out to present an almost-horizontal clump feature, without any detectable systematic effect on M_I as a function of colour or $[\text{Fe}/\text{H}]$. In fact, dividing our simulation of Fig. 6 into ‘blue’ ($V-I < 1.1$) and ‘red’ ($V-I > 1.1$) samples, we obtain values of $M_I^{\text{RC}} = -0.159$ and $M_I^{\text{RC}} = -0.170$, respectively.

How can the galaxy models present almost-horizontal clumps, whereas M_I^{RC} changes systematically as a function of both age and metallicity? The answer is not straightforward, since a number of effects enter into the game. First, M_I does not change monotonically with age: it is fainter than the mean (by up to 0.4 mag) at *both* the ~ 1 Gyr and $\gtrsim 10$ Gyr age intervals, which represent the bluest and reddest clump stars for a given metallicity (provided that Z and t are not, respectively, too low and too old, to cause the appearance of a blue HB). Due to this effect alone, the clump for a given metallicity would describe an arc in the CMD, without a detectable mean slope in the M_I versus $V-I$ CMD (see GGWS98). Second, an age-metallicity re-

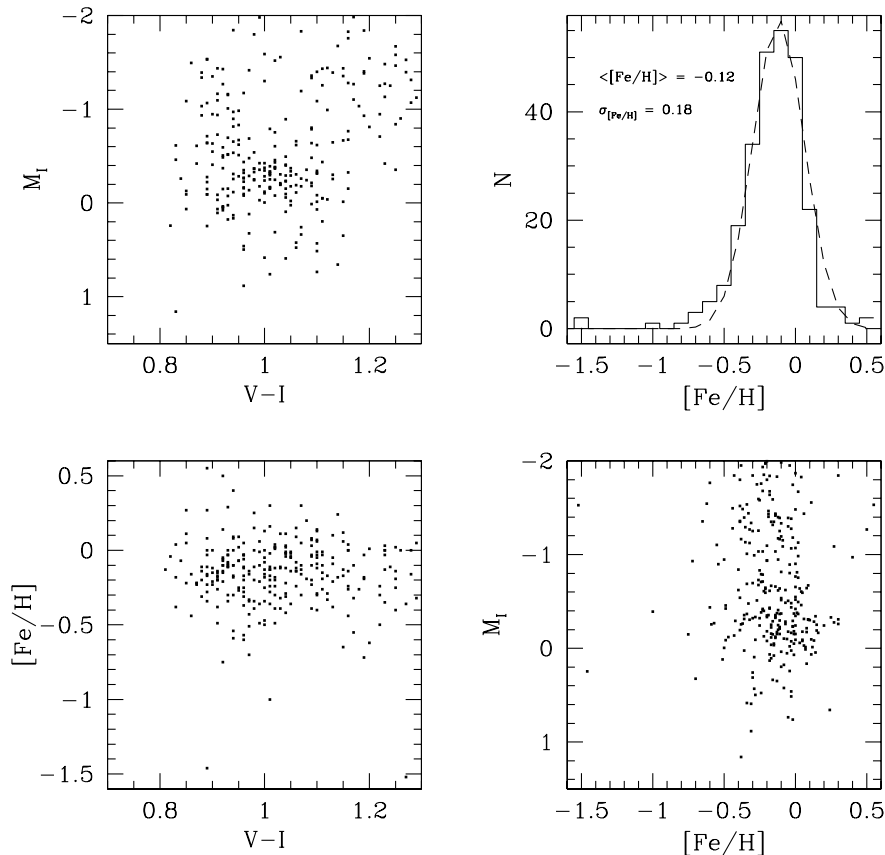


Figure 8. Metallicities of clump stars in the *Hipparcos* catalogue (see text). For the stars shown in the CMD of the upper left panel, the $[Fe/H]$ distribution (upper right panel) turns out to be well described by a Gaussian of mean -0.12 dex and dispersion 0.18 dex. The two lower panels show the same stars in the $[Fe/H]$ versus $V-I$, and M_I versus $[Fe/H]$ diagrams.

lation tends to flatten the M_I vs. age relation in the age interval $t \gtrsim 2$ Gyr, since older clump stars tend to become dimmer due to their larger age, but brighter due to the lower metallicity. Third, the presence of a ~ 0.2 dex metallicity dispersion among stars of the same age, may cause substantial blurring in the diagrams of Fig. 8. Which effect prevails depends on the exact shape of the SFR and AMRs. The important point is that, due to these effects, the possible correlations between colour, magnitude, and metallicity of clump stars, may become small enough to escape detection.

Therefore, clump models can assume a quite large variety of shapes, depending on the SFR and AMR. The position of an individual star in the CMD, in general cannot be unequivocally interpreted as the result of a given age or metallicity. There are, however, important exceptions to this rule: A quite striking feature of the models is the presence of a ‘secondary clump’ feature located about 0.4 mag below the blue extremity of the clump, accompanied by a bright plume of clump stars directly above it. These features are described in detail in GGWS98 and Girardi (1999). They are caused by the intermediate-mass clump stars, i.e. those just massive enough for starting to burn helium in non-degenerate conditions, and are the signature of $\lesssim 1$ -Gyr old populations with metallicities $Z \gtrsim 0.004$ (Girardi 1999). The important point here is that these structures are present in the *Hipparcos* CMD, and about as populated as they are in the models presented in Fig. 6. It evidences that some key aspects of the formalism and stellar models we use are correct, and that

the adopted SFR and AMR constitute a reasonably good approximation.

3.5 The magnitude as a function of $[Fe/H]$

From our simulation, we can also derive the metallicity and age distribution of local clump stars. They are presented in Fig. 9.

Although the total range of metallicities allowed by the model is very large ($-0.7 \lesssim [Fe/H] \lesssim 0.3$, see Fig. 5), the distribution for clump stars turns out to be very narrow: a Gaussian fit to the $[Fe/H]$ distribution produces a mean $\langle [Fe/H] \rangle = +0.03$ dex and dispersion $\sigma_{[Fe/H]} = 0.17$ dex. (Actually, the $[Fe/H]$ distribution presents an asymmetric tail at lower metallicities, which causes the straight mean of $[Fe/H]$ to be -0.04 dex, i.e. slightly lower than the center of the Gaussian.) This distribution is almost identical to the observed one (Fig. 8), except for an offset of $+0.15$ dex.

The small $[Fe/H]$ dispersion displayed in the lower panel of Fig. 9 is easily understood when we look at the clump age distribution in the upper panel. Not surprisingly (cf. the discussion in Sect. 3.3) the mean age of nearby clump stars turns out to be $\langle t \rangle = 2.5$ Gyr, whereas the peak of the distribution is at just 1 Gyr. At these ages, the local disc metallicity had already grown to $[Fe/H] \sim 0.0$ dex (cf. Fig. 5), and the bulk of clump stars is expected to have similar metallicities. Therefore, this main aspect of the metallicity distribution – the small $[Fe/H]$ dispersion – is very well accounted for by the models.

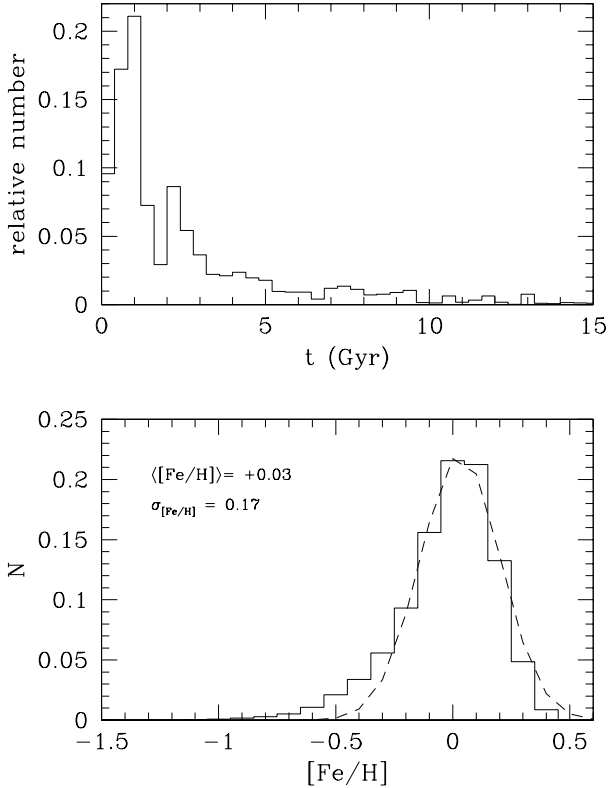


Figure 9. The distribution of ages (upper panel) and metallicities (lower panel) for clump stars in our *Hipparcos* model (continuous lines). Their mean age turns out to be 2.5 Gyr. The $[Fe/H]$ distribution is well described by a Gaussian (dashed line) of mean +0.03 dex and dispersion 0.17 dex.

The reasons for the +0.15 dex offset are not clear, and may lie in some offset between the high resolution spectroscopic $[Fe/H]$ scale by Cayrel de Strobel et al. (1997) and the one used by Rocha-Pinto et al. (2000a), or in some inconsistency between the age scales used by Rocha-Pinto et al. (2000b) and by our stellar models. As for the metallicity scale, Rocha-Pinto et al. (2000a) used the $[Fe/H]$ scale by Schuster & Nissen (1989) based on Stroemgren photometry. As discussed by Schuster & Nissen (1989) this metallicity scale is on average $\simeq 0.06$ dex lower than direct high resolutions spectroscopic $[Fe/H]$ determinations (see also Alonso et al. 1996).

Anyway, +0.15 dex may be a difference small enough to be allowed in the present work. To check this point, we make a modified *Hipparcos* model by adopting metallicities 0.15 dex lower than those given by Rocha-Pinto et al. (2000b) AMR. The clump simulated in this way becomes bluer by about 0.1 mag, if compared to the one shown in Fig. 6, and then would better agree with the range of $V-I$ colours of the observed *Hipparcos* clump (see Fig. 8). For this model, we obtain $M_I^{RC} = -0.209$ with $\sigma_{M_I} = 0.075$. Thus, a -0.15 dex change in $[Fe/H]$ scale would cause just a -0.04 mag change in the reference value of M_I^{RC} .

Fig. 10 shows the distribution of stars from our *Hipparcos* model in the $[Fe/H]$ versus $V-I$ (left panel) and M_I versus $[Fe/H]$ (right panel) planes. These occupy the same regions of these planes as the data shown in Fig. 8, apart

from the offsets of +0.15 dex in $[Fe/H]$, and +0.1 mag in $V-I$. Also the models do not show any significant correlation of $[Fe/H]$ with either $V-I$ or M_I . The only particularity is the presence of two main sequences of clump stars in the $[Fe/H]$ versus $V-I$ plane, which are due, essentially, to two main groups of clump stars: the ‘old’ ones which follow the age-metallicity relation and span the $V-I$ interval from 1.0 to 1.2, and $[Fe/H]$ from 0.0 to -0.6 ; and the youngest ones which have $[Fe/H] \gtrsim 0.0$ and concentrate at $V-I \sim 0.9 - 1.2$. With a reasonable distribution of observational errors (i.e., typical errors on the $[Fe/H]$ values are of about 0.15 dex), these two sequences can give origin to a distribution in which no general $[Fe/H]$ versus $V-I$ relation is apparent.

Udalski (2000) used the data for local clump stars to fit M_I^{RC} to data in different $[Fe/H]$ bins. The results were then used to derive the ‘metallicity dependence’ of M_I^{RC} . We can now check whether our models produce a similar relation from synthetic data. There is however, an important difference in our interpretation of this relation: in the models, it does not assume the character of a general relation, as was intended to be measured in Udalski (2000). Instead, *the M_I^{RC} versus $[Fe/H]$ relation derived in this way cannot be considered universal, because it represents the result of a very particular distribution of clump ages and metallicities* (displayed in Fig. 9).

Table 3 presents the M_I^{RC} values we derive for different $[Fe/H]$ bins in the models. They are divided in groups composed by ‘metal-poor’, ‘intermediate’, and ‘metal-rich’ bins. For each group, the final slope of the M_I^{RC} versus $[Fe/H]$ relation is also presented, both for the cases in which all bins have been included, and ignoring the metal-rich bin as in Udalski (2000). The first group represents the same bin limits as in Udalski (2000), and results in a very flat M_I^{RC} versus $[Fe/H]$ relation. The second group has bins shifted by +0.15 dex, in order to account for the offset in our models’ metallicities; in this case, a marginal slope of 0.14 ± 0.06 mag/dex is detected, which increases to 0.24 mag/dex if we consider only the metal-poor and intermediate bins.

These two former groups present too few stars in the metal-poor bin. We tried to improve upon this point, selecting bin limits such as to separate the peak and wings of the metallicity distribution shown in Fig. 9. The result is a mean slope of 0.13 ± 0.05 mag/dex.

Udalski (2000) gets a slope for the M_I^{RC} versus $[Fe/H]$ relation of about 0.2 mag/dex using all three bins in their fit, and of 0.13 ± 0.07 mag/dex considering only the metal-poor and intermediate bins. Similar results (Table 3) are obtained with our models which include an offset in the metallicity scale. However, we do not give any strong weight to the final slope resulting from the models. In fact, the present exercises convinced us that the obtained slope may depend somewhat on the way the bins are defined. Moreover, the simulation of observational errors in the models, could probably lead to slightly different results. What we have done in this section should be considered, rather than a model calibration, just a check of whether Udalski’s results can be understood with present theoretical models of clump stars.

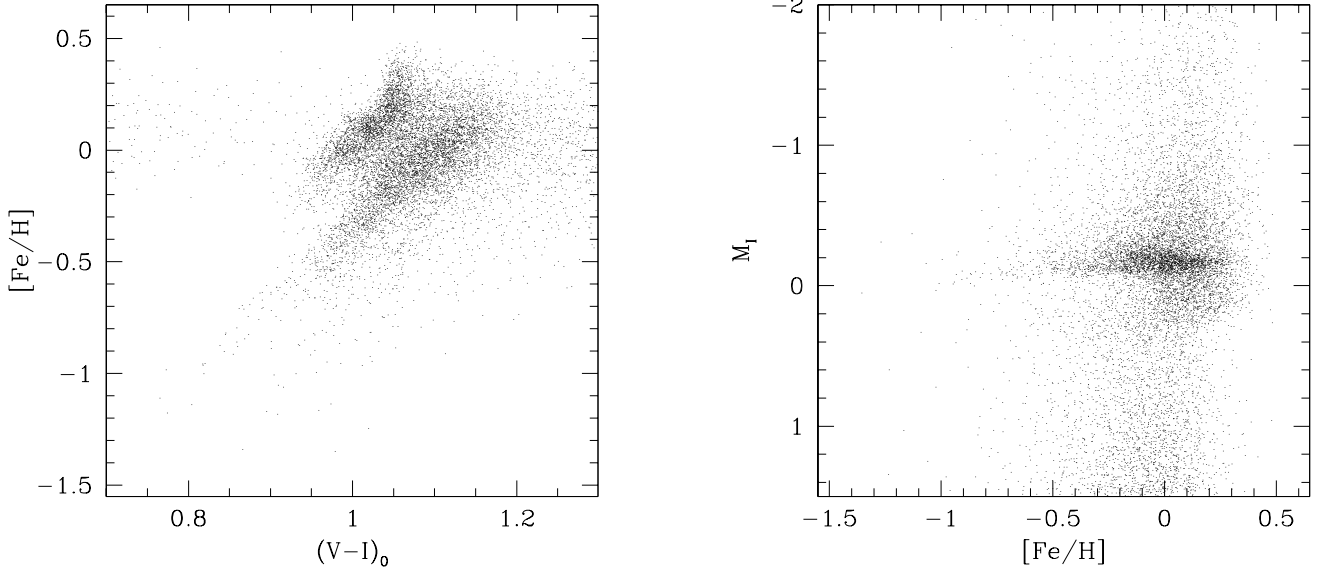


Figure 10. The distribution of stars from our *Hipparcos* model (see Fig. 6) in the $[\text{Fe}/\text{H}]$ versus $V-I$ (left panel) and M_I versus $[\text{Fe}/\text{H}]$ (right panel) planes. Compare with the observational distribution of Fig. 8.

Table 3. M_I^{RC} for *Hipparcos* model, separated in $[\text{Fe}/\text{H}]$ bins, and the derived slope of M_I^{RC} versus $[\text{Fe}/\text{H}]$.

Group	$[\text{Fe}/\text{H}]$ bin limits	M_I^{RC}	σ	clump fraction	$\langle[\text{Fe}/\text{H}]\rangle$	slope
1	-0.60, -0.25	-0.135	0.039	0.12	-0.38	-0.07 ± 0.06 (a)
	-0.25, -0.05	-0.176	0.082	0.26	-0.14	0.00 (b)
	-0.05, +0.20	-0.167	0.049	0.58	0.07	
2	-0.45, -0.10	-0.221	0.081	0.14	-0.22	0.14 ± 0.06 (a)
	-0.10, +0.10	-0.170	0.059	0.46	0.01	0.24 (b)
	+0.10, +0.35	-0.164	0.039	0.30	0.18	
3	-0.55, -0.05	-0.218	0.072	0.18	-0.21	0.13 ± 0.05 (a)
	-0.05, +0.15	-0.167	0.052	0.48	0.05	0.32 (b)
	+0.15, +0.45	-0.164	0.038	0.21	0.23	

Note: (a) Fit using all 3 bins; and (b) mean slope using only the metal-poor and intermediate bin.

4 THE CLUMP IN STAR CLUSTERS

We have seen in the previous section how theoretical models are able to reproduce the main observational features of the *Hipparcos* red clump. Another crucial test for the reliability of theoretical models involves the use of star clusters. Since star clusters are made of stars all with the same age and initial chemical composition, they constitute template single-burst stellar populations with which it is possible to compare the ΔM_I^{RC} values derived from theory. With a large sample of clusters of different ages and metallicities, we can directly test the predicted metallicity and age dependence of this key quantity. Galactic open clusters are particularly useful in this respect, since they are well studied objects with a large age range, and reasonably accurate distance and age estimates.

To this aim, we have adopted the data (ages, M_I^{RC} and $[\text{Fe}/\text{H}]$) by Sarajedini (1999) for a sample of 8 galac-

tic open clusters, plus the data from Twarog et al. (1999) for NGC 2506. The clusters span the age range between 1.9 and 9.5 Gyr, while the metallicities range between $[\text{Fe}/\text{H}] = -0.39$ and $[\text{Fe}/\text{H}] = 0.15$. Since we want to test the theoretical ΔM_I^{RC} values, for each cluster we have computed the observational ΔM_I^{RC} value using $M_I^{\text{RC}}(\text{Hipp.}) = -0.23 \pm 0.03$ (Stanek & Garnavich 1998) for the local red clump. The same quantity has been derived from the theoretical models, using for the local clump the M_I^{RC} value given in Table 4. There is a further detail we considered; since Sarajedini (1999) measured the luminosity of the peak of the red clump stellar distribution, and not its mean value, we have derived from our simulations (see discussion in Sect. 2.1) the M_I values corresponding to the peak of the red clump LF, for the relevant age and metallicity range, rather than the mean values defined in Sect. 2. We remark that the peak

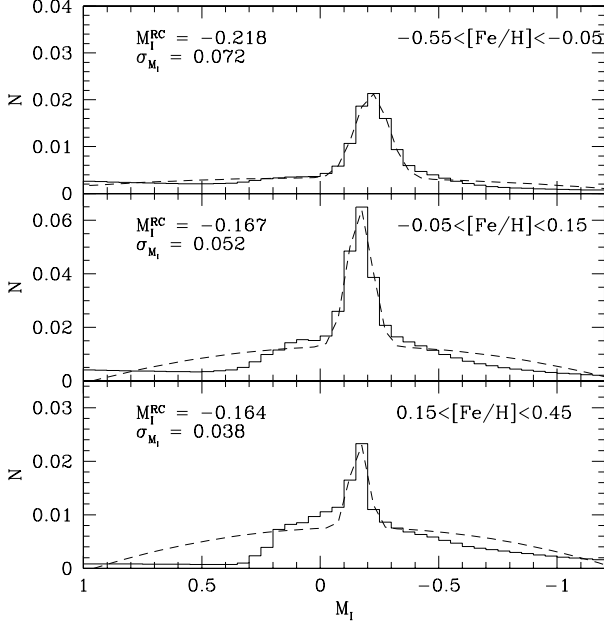


Figure 11. The LFs for clump stars in our *Hipparcos* model, separated into 3 $[\text{Fe}/\text{H}]$ bins (see text).

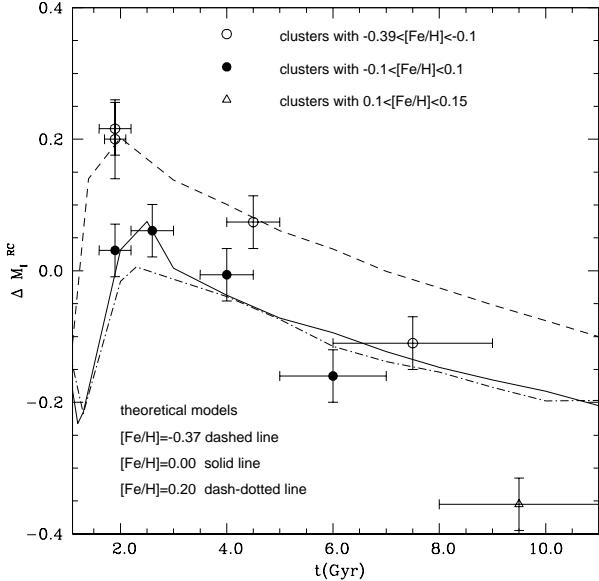


Figure 12. Comparison of theoretical ΔM_I^{RC} values with the observational counterpart in a sample of open clusters of various metallicities and ages.

values are systematically lower than mean values by about 0.06 mag.

In Fig. 12 we show the comparison between observed and theoretical ΔM_I^{RC} values. It is immediately evident how the observations show a marked dependence of ΔM_I^{RC} on the clusters' age and $[\text{Fe}/\text{H}]$ values. Moreover, it is clear that observations are well reproduced by theoretical models (with the sole exception of NGC 6791, the oldest cluster in

the plot). This lends further support to the use of theoretical models for computing ΔM_I^{RC} .

Before concluding this section we just mention that the data by Sarajedini (1999) and Twarog et al. (1999) are inconsistent with the ones by Udalski (1998b), who has shown how the M_I^{RC} value for a sample of 15 star clusters in the LMC and SMC is largely independent of age and metallicity, in the age interval from 2 to 10 Gyr. However, it is clear that the determination of metallicity and age for LMC and SMC clusters is subject to larger uncertainties than in the case of their Galactic counterparts. Moreover, additional uncertainties due to depth effects and geometric corrections (values as high as ± 0.2 mag being applied for some SMC clusters) can also spuriously modify the observed relationship between red clump brightness, metallicity and age.

Udalski (1998b) has also noticed that in the oldest clusters of his sample the clump is 0.3 – 0.4 mag fainter than the mean in the 2 – 10 Gyr interval. This observation could be simply reflecting the gradual fading of the clump, that occurs in the models for ages larger than 3 Gyr (see Fig. 12).

We conclude that the empirical evidence for a negligible dependence of the clump magnitude on age (Udalski 1998b), is weak compared to the evidence that it depends on age (Fig. 12). A larger sample of Magellanic Clouds cluster data may certainly improve upon the present-day results.

We also remark that in galaxies with recent star formation, a large fraction of the clump stars should have ages in the 1 – 2 Gyr interval (as discussed in Sect. 3.1). Clusters younger than 2 Gyr, however, are not present in Udalski's (1998b) and Sarajedini's (1999) samples. It would be extremely interesting, in future empirical works, to test the age dependence of M_I^{RC} in samples containing also younger clusters.

5 THE CLUMP IN OTHER GALAXY SYSTEMS

In Sects. 2 and 3, the main factors determining the mean clump magnitude in a galaxy model have been extensively reviewed. In the present section we proceed computing M_I^{RC} for a series of models representing nearby galaxy systems, whose mean clump magnitudes have been used in the past for distance determinations (by galaxy systems we mean composite stellar populations, whose stars cover relatively large intervals of age and metallicity). All results from this section are summarized in Table 4.

There are just two further technical details we need to mention before proceeding: (i) In all models, we assume the relation $[\text{Fe}/\text{H}] = \log(Z/0.019)$, which is appropriate for populations with scaled-solar distributions of metals. The case of stars with enhancement of α -elements will be discussed in Sect. 5.5. (ii) For the few cases in which tracks with metallicities lower than $Z = 0.0004$, or higher than $Z = 0.03$ are required, we use these two limiting values. This is done to avoid risky extrapolations of the model behaviours. Anyway, apart from the case of the Carina dSph galaxy, stars with such extreme metallicities represent just a tiny fraction of the clump stars in our models.

Table 4. M_I^{RC} and mean [Fe/H] values for the clump in nearby galaxy systems.

System	SFR(t)	AMR	M_I^{RC}	ΔM_I^{RC}	[Fe/H] ^{RC}	comm.
Solar Neighbourhood (<i>Hipparcos</i>)	Rocha-Pinto et al. (2000b)	Rocha-Pinto et al. (2000a)	−0.171	0.000	−0.04	(★)
Baade’s Window (solar-scaled)	8 – 12 Gyr old Mollá et al. (2000)	McWilliam & Rich (1994) Mollá et al. (2000)	−0.087 −0.063	−0.084 −0.108	−0.22 −0.36	(★) (1)
Baade’s Window (α -enhanced)	8 – 12 Gyr old Mollá et al. (2000)	McWilliam & Rich (1994) Mollá et al. (2000)	−0.161 −0.148	−0.010 −0.023	−0.22 −0.36	(★) (1)
Carina dSph	Hernandez et al. (2000a) Hurley-Keller et al. (1998) best model	[Fe/H] = −1.7 [Fe/H] = −1.7	−0.458 −0.271	+0.287 +0.100	−1.7 −1.7	(★) (2)
SMC	Pagel & Tautvaišienė (1998)	Pagel & Tautvaišienė (1998)	−0.457	+0.286	−0.77	(3, ★)
LMC bar	Holtzman et al. (1999; their fig. 2) Holtzman et al. (1999; their fig. 4) Holtzman et al. (1999; their fig. 11)	Pagel & Tautvaišienė (1998) Pagel & Tautvaišienė (1998) Pagel & Tautvaišienė (1998)	−0.371 −0.373 −0.386	+0.200 +0.202 +0.215	−0.39 −0.39 −0.40	(★)
LMC outer fields	Holtzman et al. (1999; their fig. 3) Holtzman et al. (1999; their fig. 5) Holtzman et al. (1999; their fig. 12)	Pagel & Tautvaišienė (1998) Pagel & Tautvaišienė (1998) Pagel & Tautvaišienė (1998)	−0.360 −0.360 −0.396	+0.189 +0.189 +0.225	−0.37 −0.37 −0.38	
LMC northern fields	Dolphin (2000)	Dolphin (2000)	−0.281	+0.110	−0.88	(4)

(★) The most representative or ‘preferred’ value of ΔM_I^{RC} for distance determinations.

(1) Theoretical model for the bulge.

(2) The clump LF is double, resulting in a bad fit of eq. 1. Their second and third best models give identical results.

(3) SFR comes from a theoretical model.

(4) This model produces a CMD with far too many old metal-poor stars.

5.1 The Baade’s Window clump

Determining the ages of Bulge stars is difficult, and so its age distribution has been somewhat uncertain. Whereas there are some indications for the presence of intermediate-mass stars (see Rich 1999 for a review), studies of Baade’s Window population (e.g. Frogel 1988; Holtzman et al. 1993; Ortolani et al. 1995; Ng et al. 1996) generally indicate that the bulk of star formation occurred at old ages. Only the very central regions of the Bulge show unequivocal evidences of recent star formation (e.g. Frogel, Tiede & Kuchinski 1999; Figer et al. 1999).

Let us then assume that the bulk of stellar populations in the Bulge are older than 5 Gyr. After this age, the clump magnitude fades slowly (only ~ 0.025 mag/Gyr), and $N_{\text{cl}}(t)$ becomes almost flat (i.e. the age distribution of clump giants become simply proportional to the SFR, as seen in Fig. 1). Therefore, the assumptions about the actual SFR history affect much less M_I^{RC} for such a population, than in the case of galaxies with ongoing star formation.

We compute two models for the Bulge (or Baade’s Window), illustrated in Fig. 13: The first assumes an ‘old’ Bulge, with constant SFR between 8 and 12 Gyr ago, and the McWilliam & Rich (1994) distribution of [Fe/H] values at any age. The latter has been obtained from spectroscopic analysis of Bulge K giants. Our second model comes from the recent ‘bulge model’ by Mollá, Ferrini & Gozzi (2000): it represents still a predominantly old Bulge, but with an ever-decreasing SFR going up to the present days. The [Fe/H](t) relation is derived from their chemical evolution models,

and is shown (Mollá et al. 2000) to produce a distribution of [Fe/H] values very similar to the observational one by McWilliam & Rich (1994).

In both cases, Bulge models show an almost-horizontal clump – in very good agreement with the observational CMD presented by Paczyński & Stanek (1998) – very extended in colour and almost evenly populated along the colour sequence (Fig. 13). Also in both cases, Bulge M_I^{RC} values turn out to be very similar, and about 0.1 mag higher (i.e. fainter) than the local *Hipparcos* ones (Table 4).

Notice that the mean metallicity of clump stars is rather similar in the local and Bulge samples (Table 4). Therefore, the fainter clump we find in Bulge models is, essentially, the result of their higher mean ages, compared to local clump stars.

5.2 The clump in the Carina dSph

The Carina dSph galaxy represents an interesting case, because of its very low metallicity, of mean [Fe/H] = −1.9 and 1σ dispersion of 0.2 dex (Mighell 1997). Moreover, its CMD clearly indicates episodic star formation (Smecker-Hane et al. 1996), with main bursts occurring ~ 15 , 7, and 3 Gyr ago (Hurley-Keller, Mateo & Nemeč 1998).

Weighting these 3 different episodes of star formation in different proportions, and with different durations, Hurley-Keller et al. (1998) find several solutions for the SFR history of Carina. We have tested their best model (first entry in their table 7), assuming metallicity values equal to

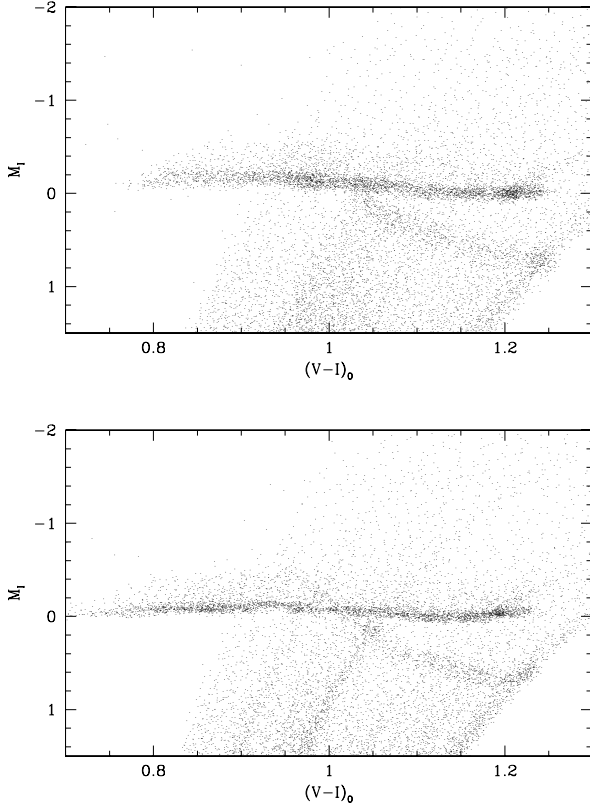


Figure 13. The same as Fig. 6, but for the Bulge, as derived from two different models: (upper panel) an ‘old’ model with constant SFR between 8 and 12 Gyr and the McWilliam & Rich (1994) [Fe/H] distribution at any age, and (lower panel) a model following the SFR and AMR from the bulge theoretical model from Mollá et al. (2000).

$Z = 0.0004$ ($[\text{Fe}/\text{H}] = -1.7$) at any age. Actually, we have tested Hurley-Keller et al.’s three best models, obtaining always identical results for M_I^{RC} .

In addition, we have tested the SFR history derived by Hernandez, Gilmore and Valls-Gabaud (2000a). They apply an objective numerical algorithm to find the SFR which best fits the observed CMD, without imposing artificial or subjective constraints on it. Their solution is characterized by periods of marked star formation separated by lower (but not null) activity. Similar results have been obtained by Mighell (1997), who also uses a non-parametric approach.

We present, in Figs. 15 and 16 the synthetic CMDs and LFs, respectively, obtained from Hernandez et al.’s (2000a) solution, and from Hurley-Keller et al.’s (1998) best model. It can be noticed (Table 4) that the two models provide M_I^{RC} values differing by 0.18 mag. Actually, there is an obvious problem in the LF fit obtained from Hurley-Keller et al.’s model: since it presents a kind of dual clump – resulting from their assumption of discrete bursts of star formation separated by periods of quiescence – the LF is badly suited for a fit with a Gaussian function. Such a fit turns out to favour the fainter clump, and clearly does not represent in a satisfactory way the magnitude distribution of clump stars. Moreover, there is no evidence of a dual clump in the observational data (e.g. figure 6 in Udalski 1998a). The clump

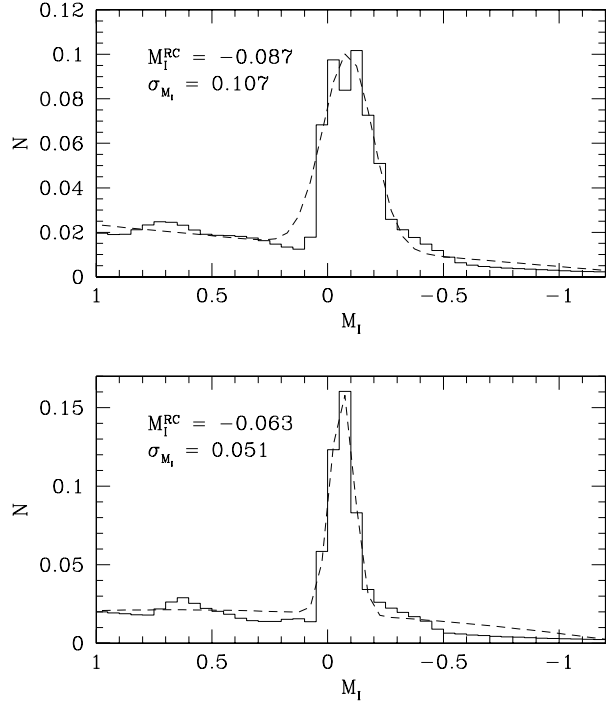


Figure 14. The same as Fig. 7, but for the Bulge models presented in Fig. 13.

obtained from Hernandez et al.’s (2000a) SFR, on the contrary, turns out to be very compact in the CMD, in better agreement with the data. For these reasons, this latter model is to be preferred in the present work.

5.3 The clump in the SMC

In the literature for the SMC, we did not find quantitative assessments of the SFR, derived directly from SMC data. Qualitative descriptions can be found in e.g. Westerlund (1997) and Hatzidimitriou (1999).

Pagal & Tautvaisiene (1998) describe both the SFR and AMR of the SMC population by means of a chemical evolution model. Their AMR is shown to describe quite well the data for SMC star clusters. Their SFR, however, is not derived directly from stellar data (as in the cases previously discussed), and hence should be looked upon with some caution. It is characterised by strong star formation in the last 4 Gyr of the SMC history, an almost negligible SFR between 4 and 10 Gyr ago, and more pronounced SFR at 10–12 Gyr.

Simulations of the SMC clump, using Pagal & Tautvaisiene (1998) results, are shown in Figs. 17 and 18. This model produces a compact clump in the CMD, but with some substructures which are due the discontinuous SFR history.

5.4 The clump in the LMC

Quantitative determinations of the SFR in the LMC abound in the literature (Bertelli et al. 1992; Vallenari et al. 1996; Holtzman et al. 1997; Stappers et al. 1997; Elson, Gilmore

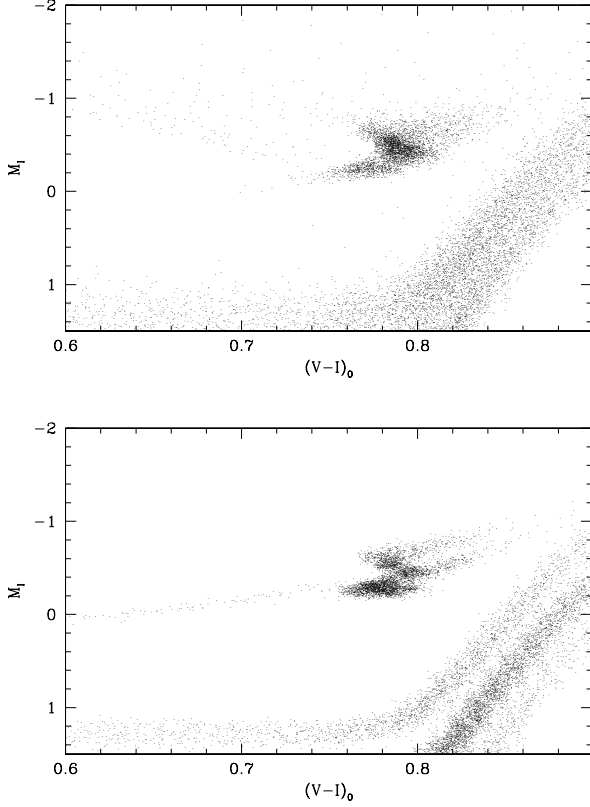


Figure 15. The same as Fig. 6, but for the Carina dSph galaxy, as derived from the SFRs and AMRs from (upper panel) Hernandez et al. (2000a), and Hurley-Keller et al. (1998) best model (lower panel).

& Santiago 1997; Geha et al. 1998). The most recent determinations are generally based on deep photometry of some few selected fields, and on fairly objective algorithms for reconstructing the SFR history (see e.g. Holtzman et al. 1999; Olsen 1999; Dolphin 2000 and references therein). A general result is that the SFR has increased in the last few Gyr (starting 2.5 – 4 Gyr ago). This increase roughly coincides with the start of a major period of formation of star clusters, and with a major increase in the stellar mean metallicities (see Olszewski, Suntzeff & Mateo 1996; Dopita et al. 1997).

In the present work, we use the SFR results from Holtzman et al. (1999). Their results correspond to two LMC regions (bar, and ‘outer’) and three different assumptions in the analysis. Namely, the following three cases have been tested by Holtzman et al.: (i) at any age, the metallicity follows a known AMR; (ii) at any age, the metallicity is not constrained; (iii) the metallicity follows a known AMR, and there has been no star formation between 4 and 10 Gyr ago. For any of the 6 different SFRs from Holtzman et al. (1999), we have to assume some AMR; we take the Pagel & Tautvaišienė (1998) one, which is known to reproduce reasonably well the AMR derived from LMC star clusters.

We show in Figs. 19 and 20 the simulations of the bar and the outer field, with the SFR derived according to item (i) above. For the same fields, (ii) and (iii) produce similar results (see Table 4).

Remarkable in the CMD of Fig. 19, is the complex struc-

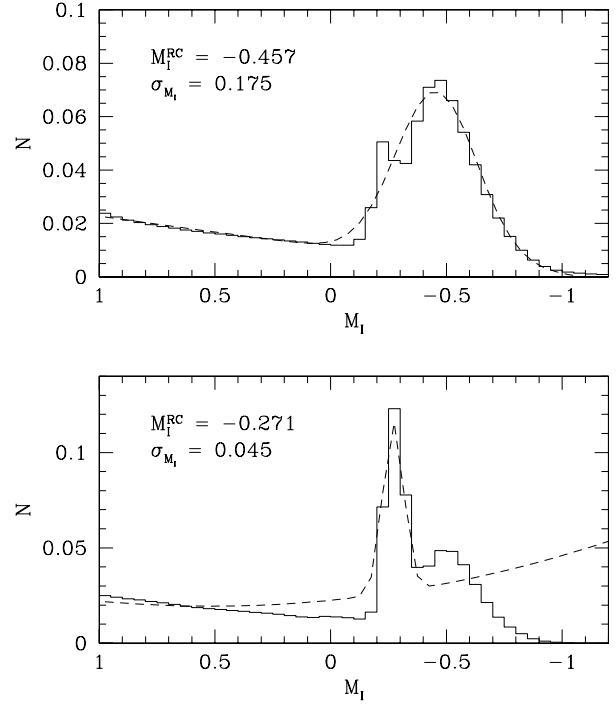


Figure 16. The same as Fig. 7, but for the Carina dSph galaxy models presented in Fig. 15.

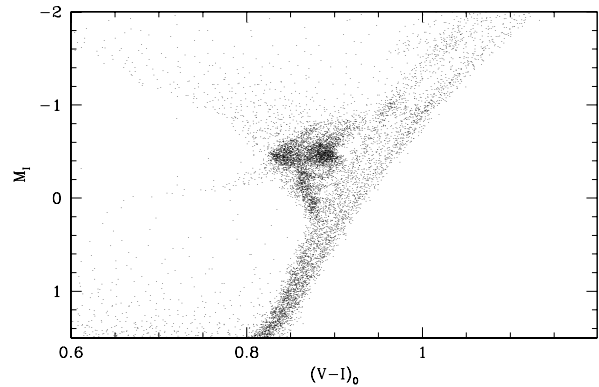


Figure 17. The same as Fig. 6, but for the SMC galaxy, as derived from the SFRs and AMRs from Pagel & Tautvaišienė (1998).

ture of the predicted LMC clump. It presents a marked vertical structure on the blue side, starting about 0.4 – 0.5 mag below the mean clump, and extending to higher luminosities. This feature of the models (the ‘secondary clump’; or ‘vertical structure’) has been extensively discussed by Girardi (1999), and has been clearly observed in some outer LMC fields by Bica et al. (1998) and Piatti et al. (1999). Moreover, the simulated LMC clumps present a horizontal tail of stars departing to the blue, which is simply the beginning of the old and metal-poor horizontal branch. It is interesting to notice the extreme similarity between these simulated clumps (Fig. 19), and the detailed CMD of a large area in

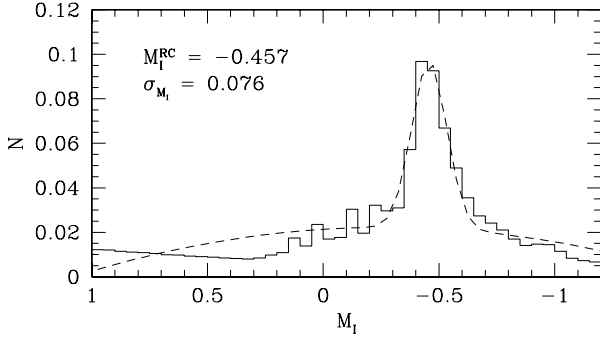


Figure 18. The same as Fig. 7, but for the SMC model presented in Fig. 17.

the northern LMC presented by Piatti et al. (1999, their figure 4).

Finally, we have also tested the SFR and AMR derived by Dolphin (2000) from a field in the northern LMC. Surprisingly, this simulation produces a double clump (Fig. 19), which is evidently the result of a large population of old metal-poor stars in Dolphin’s (2000) solution. The synthetic CMDs turn out not to reproduce the characteristics of the LMC clump, as noticed by Dolphin himself. Moreover, the mean $[\text{Fe}/\text{H}]$ of clump stars is -0.88 dex for this model, which is far too low if compared with typical values found for LMC field giants. For these reasons, we prefer not to use the results from this latter model in our analysis.

5.5 Considering the enhancement of α -elements

All the models discussed above assume a scaled-solar distribution of metals. However, it is well established that in some stellar populations (e.g. the Galactic Halo) the group of α -elements (mainly O, Ne, Mg, Si, Ca, Ti) is overall enhanced with respect to Fe in comparison with solar ratios (i.e. $[\alpha/\text{Fe}] > 0$). This is probably the case for Bulge giants, where measurements of Mg and Ti abundances provide an enhancement by about $+0.4$ dex (see McWilliam & Rich 1994; Barbuy 1999). This is usually considered to be evidence for the chemical enrichment in the Bulge having occurred in a relatively short time scale.

A ratio $[\alpha/\text{Fe}] = 0.4$ means that, at a given $[\text{Fe}/\text{H}]$ value, the metal content Z is a factor of about 2.5 larger than given by the scaled-solar relation $[\text{Fe}/\text{H}] = \log(Z/0.019)$. Moreover, for nearly-solar metallicities, α -enhanced models cannot be reproduced by scaled-solar ones by simply modifying the relationship between Z and $[\text{Fe}/\text{H}]$ (Salaris & Weiss 1998; Salasnich et al. 2000). Therefore, it is worth exploring how the Bulge M_I^{RC} would change if appropriate α -enhanced models were adopted. To this aim, we repeated our Bulge simulations using the isochrones from Salasnich et al. (2000), for both scaled-solar and α -enhanced ($[\alpha/\text{Fe}] \simeq 0.35$ dex) cases. The difference between both M_I^{RC} values was then added to the value obtained from Girardi et al.’s (2000) scaled-solar models (see Table 4).

It turns out that α -enhanced models produce a Baade’s Window clump about 0.08 mag brighter than the scaled-solar ones. This occurs because of two competing effects. For the same $[\text{Fe}/\text{H}]$ distributions centered at almost-solar

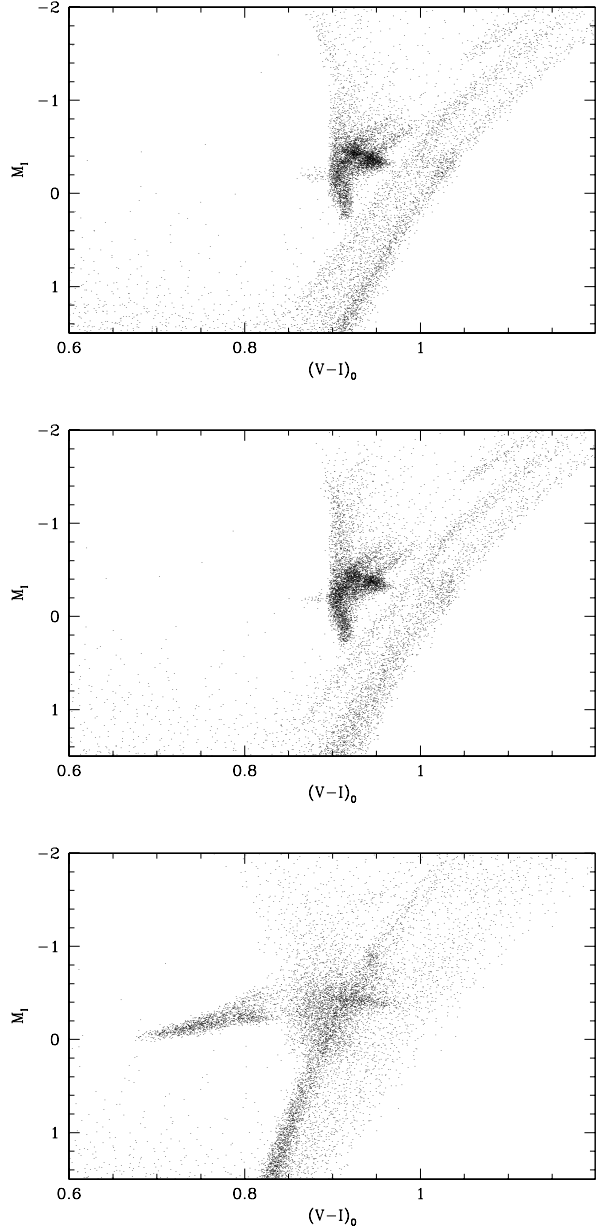


Figure 19. The same as Fig. 6, but for the LMC, as derived from Holtzman et al.’s (1999; their figure 2) bar field (upper panel), from Holtzman et al.’s (1999; their figure 3) outer fields (middle panel), and from Dolphin (2000) outer fields (lower panel).

values ($[\text{Fe}/\text{H}] \sim -0.2$ dex; see Table 4), α -enhanced models have a much higher Z , and higher Z causes lower clump brightness at a given age. However, since our models assume a constant helium-to-metals enrichment ratio of 2.25, much higher values of the helium content Y are reached by the α -enhanced models; due to the fact that an increase of Y (at fixed age and Z) causes an increase of the clump brightness, the net effect of using α -enhanced models is an increase of the clump luminosities with respect to the scaled-solar case. The final result is that Bulge models computed considering the enhancement of α elements, may have M_I^{RC} values very similar to those of the *Hipparcos* sample.

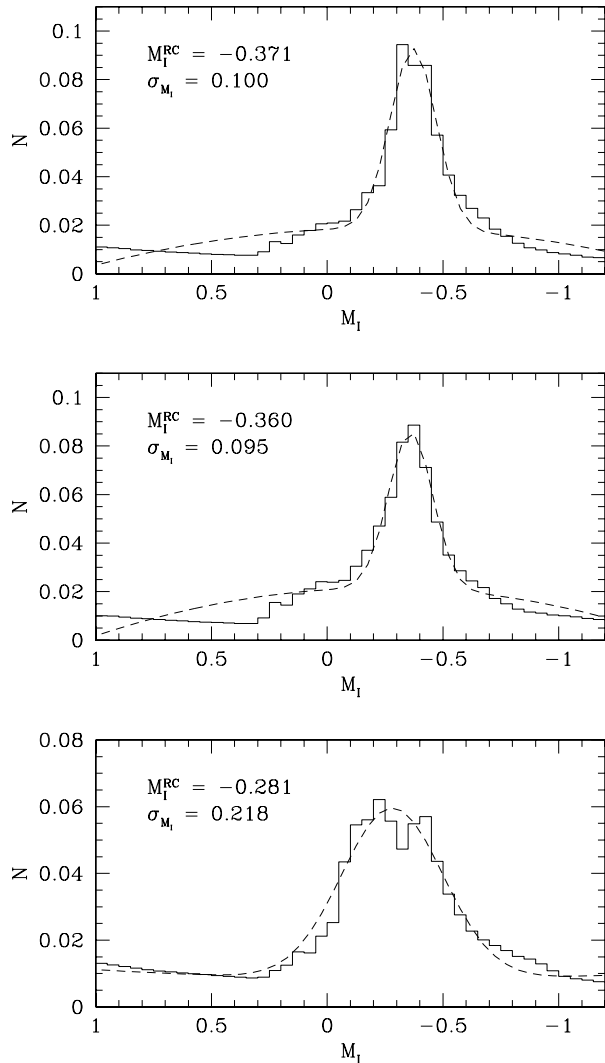


Figure 20. The same as Fig. 7, but for the LMC models presented in Fig. 19.

In the other galaxies we are considering, α -enhancement should not be as important as in the Bulge. In the cases of the Solar Neighbourhood and the Magellanic Clouds, the bulk of clump giants are relatively young ($\lesssim 3$ Gyr), and such stellar populations are expected to have a scaled-solar metal distribution. This is confirmed by spectroscopic observations of: (i) thin disk stars, that indicate almost scaled-solar ratios ($[\text{Mg}/\text{Fe}]$ between 0.0 and 0.1 dex) for stars with $[\text{Fe}/\text{H}] > -0.5$ (Fuhrmann 1998); and (ii) giants in LMC clusters younger than 3 Gyr and with $[\text{Fe}/\text{H}] \sim -0.5$, which have $[\text{O}/\text{Fe}] \sim +0.1$ dex (Hill et al. 2000). These low levels of α -enhancement can, at least as a first approximation, be ignored.

The situation for the Carina dSph is not clear. The clump giants in this galaxy are neither too young, nor have been formed in a short time interval as the Bulge ones. Thus, it is not clear whether some degree of α -enhancement should be expected, and present observations do not give information on this. Thus, we prefer not to consider the possibility of α -enhancement for this galaxy.

5.6 The clump – RR Lyrae difference

Udalski (1998a) measured the mean clump apparent magnitude I_0^{RC} in Baade’s Window, LMC, SMC, and Carina dSph galaxy. For the same fields, RR Lyrae data has provided a reference magnitude to compare the clump with. Assuming that RR Lyrae stars follow a $M_V^{\text{RR}} = (0.18 \pm 0.03)[\text{Fe}/\text{H}] + \text{const}$ relation and adopting empirical mean values for the metallicity of RR Lyrae in the different environments, Udalski (1998a) constructed the $I_0^{\text{RC}} - V_0^{\text{RRatGB}}$ parameter, where V_0^{RRatGB} means the magnitude that RR Lyrae in each galaxy would have if they had the same $[\text{Fe}/\text{H}]$ as the Bulge ones. Udalski’s (1998a) data for Baade’s Window has been later revised by Popowski (2000). Following the results by Paczyński et al. (1999) about a systematic difference between OGLE-I and OGLE-II photometry, he considers a clump dimmer by 0.035 mag with respect to Udalski (1998a) data and RR Lyrae stars brighter by 0.021 mag; this produces a change of $I_0^{\text{RC}} - V_0^{\text{RRatGB}}$ by +0.06 mag. Moreover, in order to solve the so-called ‘ $V-I$ colour problem’ of Baade’s Window clump giants (Paczynski 1998), Popowski (2000) modifies the original extinction values and reddening curves for Baade’s Window by an amount which implies a final global revision by +0.17 mag for the $I_0^{\text{RC}} - V_0^{\text{RRatGB}}$ value.

By construction, $I_0^{\text{RC}} - V_0^{\text{RRatGB}}$ provides the differential behaviour of M_I^{RC} in these four stellar systems, and it is therefore interesting to compare it with the $\Delta M_I^{\text{RC}} = M_I^{\text{RC}}(\text{Hipp}) - M_I^{\text{RC}}(\text{galaxy})$ values derived from our simulations. Before proceeding, we just mention that our ZAHB models of low metallicity at $\log T_{\text{eff}} = 3.85$ (a typical average temperature for RR Lyrae stars) have the same slope of $\Delta M_V^{\text{RR}}/\Delta[\text{Fe}/\text{H}] = 0.18$ mag/dex that has been used by Udalski (1998a) to correct his RR Lyrae data. This slope is also in good agreement with the results from independent evolutionary models (see, e.g., Salaris & Weiss 1998) and from the main sequence fitting technique (Gratton et al. 1997).

The result of the comparison is shown in Fig. 21. We have used the Udalski (1998a) data and error bars, and the correction by Popowski (2000) for the Baade’s Window population. The ΔM_I^{RC} values come from Table 4. The solid line indicates a straight line of slope -1 (increasing ΔM_I^{RC} means decreasing $M_I^{\text{RC}}(\text{galaxy})$, which should correspond to a decrease of $I_0^{\text{RC}} - V_0^{\text{RRatGB}}$). It is evident that the differential behaviour of the theoretical ΔM_I^{RC} values for these four systems is in good agreement with the empirical behaviour of M_I^{RC} as provided by the $I_0^{\text{RC}} - V_0^{\text{RRatGB}}$ parameter. This occurrence, together with the agreement between theoretical and empirical ΔM_I^{RC} absolute values for the open clusters of Fig. 12, provides strong observational support to the the population corrections predicted by stellar models.

We have also tested if significant changes in this comparison are introduced when using different measures of either I_0^{RC} or V_0^{RR} . In particular, we have considered the determinations of the LMC I_0^{RC} by Romaniello et al. (2000), V^{RR} for Carina from Kuhn, Smith & Hawley (1996) – dereddened using the same reddening as in Udalski (1998a) – and the revised values of V_0^{RR} for both LMC and SMC from Udalski et al. (1999). The satisfactory agreement between the differential behaviour of the theoretical ΔM_I^{RC} and $I_0^{\text{RC}} - V_0^{\text{RRatGB}}$ is not sensibly altered.

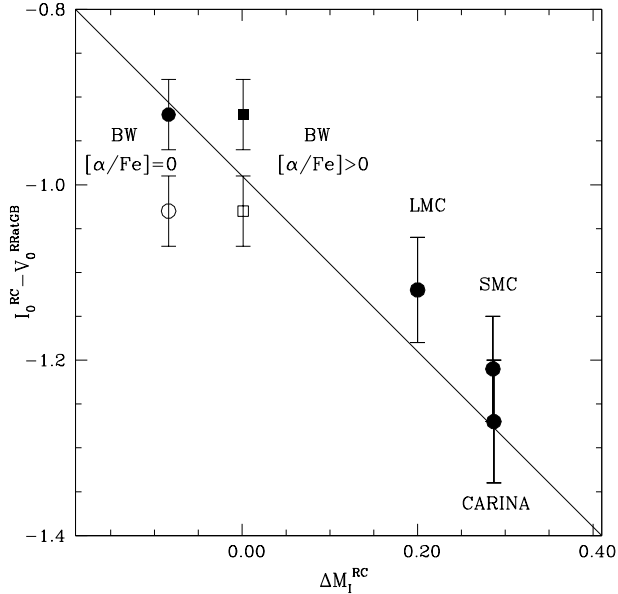


Figure 21. Observed $I_0^{\text{RC}} - V_0^{\text{RRatGB}}$ as a function of the modelled ΔM_I^{RC} values for the stellar systems of Table 4 (full circles). $I_0^{\text{RC}} - V_0^{\text{RRatGB}}$ comes from Udalski (1998a), but for the Baade’s Window point that has been revised upward in magnitude by Popowski (2000). The full line represents a straight line of slope -1 . The open symbols show the Baade’s Window data corrected only by the zero point difference between OGLE-I and OGLE-II V - and I -band magnitudes (see text for details). Squares represent models computed for the Baade’s Window adopting an α -enhanced metal distribution.

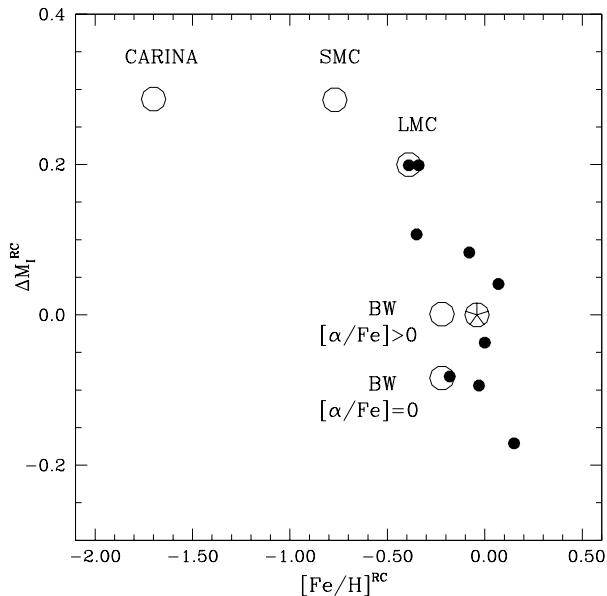


Figure 22. ΔM_I^{RC} as a function of the red clump mean $[\text{Fe}/\text{H}]$ for the stellar systems in Tab. 4 (large open circles) and the open clusters displayed in Fig. 12 (full circles). The point corresponding to the *Hipparcos* red clump (starred circle) is also plotted. Two data points are shown for the Baade’s Window clump, corresponding to the results obtained with either scaled-solar or α -enhanced models.

In Fig. 22 we show the run of ΔM_I^{RC} as a function of the mean red clump $[\text{Fe}/\text{H}]$ for the stellar systems in Tab. 4, the local *Hipparcos* red clump and the open clusters of Fig. 12. If we consider, for example, metallicities around $[\text{Fe}/\text{H}] = -0.1$ one can easily notice the large dispersion of the ΔM_I^{RC} values. On the basis of all the evidences discussed in this paper it is easy to understand that this dispersion is due to the different SFR and AMR of the stellar populations we are considering. This should also warn against the use of empirical linear relationships for deriving ΔM_I^{RC} as a function of $[\text{Fe}/\text{H}]$. ΔM_I^{RC} depends in a complicated way on the properties of the stellar populations under scrutiny and any empirical calibration of this quantity is not universal, but reflects the particular SFR and AMR of the calibrating sample. Moreover, there is no physical reason at all for linear relationships to hold for ΔM_I^{RC} .

If we consider only the stellar systems of Tab. 4 and try to fit a linear relationship to the points displayed in Fig. 22 (open circles) we would derive a slope of about 0.18, in agreement with the slope of the empirical corrections (0.19 ± 0.05) derived by Popowski (2000) using the $I_0^{\text{RC}} - V_0^{\text{RRatGB}}$ values as a function of $[\text{Fe}/\text{H}]$ for the same sample of objects; but we want to stress the point that this slope has no meaning whatsoever. It is just an accident that for this particular sample of galaxies there is a relationship close to a linear one between the clump brightness and the metallicity. In distance determinations, the individual values of ΔM_I^{RC} derived from population synthesis simulations must be used, and not an average relation obtained from a linear fit to the real corrections.

6 CONCLUSIONS ABOUT THE CLUMP DISTANCE SCALE

In the previous two sections we have shown how theoretical models of stellar populations are able to reproduce most of the relevant observational features regarding red clump stars in different environments. In the following we will redetermine the red clump distances to the galactic and extragalactic systems previously discussed using I_0^{RC} values taken from the literature. It is not our intention to exhaustively discuss the uncertainties and conflicting results about the distances to these stellar systems; we only want to show the changes of the distance estimates using red clump stars when one is using the ΔM_I^{RC} corrections predicted by stellar models.

6.1 The Bulge – Magellanic Clouds – Carina dSph distance scale

By applying the red clump method (see Eq. 1) and the population corrections ΔM_I^{RC} displayed in Table 4, we derive here the distances to the Galactic Bulge, LMC, SMC and Carina dSph. The values for I_0^{RC} and A_I come from the literature, and $M_I^{\text{RC}} = -0.23 \pm 0.03$ (Stanek & Garnavich 1998) has been empirically obtained from local *Hipparcos* red clump stars.

By using a dereddened $I_0^{\text{RC}} = 14.32 \pm 0.04$ for the Galactic Bulge (Udalski 1998a) and $\Delta M_I^{\text{RC}} = -0.087$ (from solar-scaled models; Table 4), using the McWilliam & Rich (1994) AMR, we get $\mu_0^{\text{GB}} = 14.47 \pm 0.05$. Analogous value is obtained using the SFR and AMR by Mollá et al. (2000). It

corresponds to a linear distance of 7.8 ± 0.2 Kpc, in good agreement with the generally accepted value of the distance to the Galactic center 8.0 ± 0.5 Kpc (Reid 1993). Our estimate, however, is slightly lower than the values obtained by Paczyński & Stanek (1998) and Stanek & Garnavich (1998), simply because we include a population effect which was then assumed to be negligible. If instead we correct I^{RC} by $+0.035$ mag as suggested by Paczyński et al. (1999) and Popowski (2000), and modify A_I by -0.11 mag as suggested by Popowski (2000), we get $\mu_0^{\text{GB}} = 14.62 \pm 0.05$ (8.4 ± 0.2 Kpc). These results slightly change if we consider the α -enhanced model for the Bulge. In this case the population effect is negligible and we obtain, respectively, $\mu_0^{\text{GB}} = 14.55 \pm 0.05$ (8.1 ± 0.2 Kpc) and $\mu_0^{\text{GB}} = 14.70 \pm 0.05$ (8.7 ± 0.2 Kpc).

In the case of the LMC there is still much debate about the observational value of the red clump I_0^{RC} (Zaritsky 1999; Romaniello et al. 2000; Udalski 2000), the main reason being the extinction correction (see also Sec. 1). Romaniello et al. (2000) obtained $I_0^{\text{RC}} = 18.12 \pm 0.02$, a value in agreement also with the results by Zaritsky (1999), while Udalski (2000) obtained $I_0^{\text{RC}} = 17.94 \pm 0.05$. When adopting Romaniello et al.'s (2000) result, together with $\Delta M_I^{\text{RC}} = 0.200$ (considering the SFR from figure 2 of Holtzman et al. 1999; see Table 4), we get a LMC distance modulus $\mu_0 = 18.55 \pm 0.05$ (51.3 ± 1.1 Kpc). The other SFR prescriptions by Holtzman et al. (1999) displayed in the Table 4 do not significantly modify ΔM_I^{RC} . Our μ_0^{LMC} value is in good agreement with the so-called ‘long’ distance scale. In case of assuming the Udalski (2000) dereddened red clump brightness one obtains $\mu_0 = 18.37 \pm 0.07$ (47.2 ± 1.5 Kpc). Notice that this value is ‘longer’ by 0.13 mag with respect to the result obtained by Udalski (2000) using the same red clump brightness but his empirical correction for metallicity effects.

As for the SMC Udalski (1998a) gives $I_0^{\text{RC}} = 18.33 \pm 0.05$ which, together with $\Delta M_I^{\text{RC}} = 0.286$ obtained from Table 4, provides $\mu_0^{\text{SMC}} = 18.85 \pm 0.06$ (58.9 ± 1.6 Kpc).

The distance to Carina turns out to be $\mu_0^{\text{Car}} = 19.96 \pm 0.06$ (98.2 ± 2.7 Kpc) when using $I_0^{\text{RC}} = 19.44 \pm 0.04$ from Udalski (1998a) and $\Delta M_I^{\text{RC}} = 0.287$ from Table 4 (using the Hernandez et al. 2000a SFR).

6.2 Final comments

In this paper, we use an extended set of stellar models, standard population synthesis algorithms, and independent data about the distributions of stellar ages and metallicities, to derive the behaviour of the clump magnitude in different stellar systems. We also provide the basic equations and tables for a straightforward computation of the red clump mean brightness for any stellar system.

We are able to reproduce quite well a number of observational features of the clump in nearby galaxy systems. The most striking are:

(i) *For the Hipparcos clump:* a) the distribution in the M_I versus $V-I$ diagram (a colour shift of 0.1 mag being probably due to a mismatch between two different empirical metallicity/age scales); b) the narrow and Gaussian-like $[\text{Fe}/\text{H}]$ distribution; c) the absence of a correlation between $V-I$ colour and $[\text{Fe}/\text{H}]$; d) the approximate slope of the empirical M_I^{RC} versus $[\text{Fe}/\text{H}]$ relation.

(ii) *For the Baade’s Window clump,* the wide and nearly horizontal clump in the M_I versus $V-I$ diagram.

(iii) *For the LMC,* the striking vertical structure (fainter secondary clump plus bright tail) at the blue side of the clump, and a blue plume of horizontal branch stars.

(iv) *For the SMC and Carina dSph,* the compact clump structure.

(v) *For galactic open clusters older than 2 Gyr,* the rate of change of the clump brightness with both age and metallicity.

(vi) *For the Bulge, Magellanic Clouds, Carina dSph,* the approximate slope of the empirical M_I^{RC} versus $[\text{Fe}/\text{H}]$ relation.

We have shown that the models predict a complex dependence of the red clump magnitude on age, metallicity, and star formation history, which cannot be expressed by relations such as: (i) a linear M_I^{RC} versus $[\text{Fe}/\text{H}]$ relation, or (ii) a linear (or constant) M_I^{RC} versus age relation. *Present empirical linear M_I^{RC} versus $[\text{Fe}/\text{H}]$ relations, used to describe the dependence of the red clump M_I^{RC} on the metallicity, are misleading, since they are originated by the particular age and metallicity distributions of the objects included in the calibrating sample, and do not have a general validity.* Using such linear relations may produce spurious results, even when statistically good fits to the calibrating data are obtained.

To summarize, there are four main features indicated by the models, that cannot be expressed by present empirical relations:

(i) M_I^{RC} depends on both metallicity and age, and then on the underlying age-metallicity relation;

(ii) for a given metallicity, the M_I^{RC} versus age relation is complex and not monotonic;

(iii) at a given age, M_I^{RC} generally increases with $[\text{Fe}/\text{H}]$, but not necessarily in a linear way;

(iv) stars of different ages have very different weights in determining M_I^{RC} in a galaxy, younger stars (if present) being dominant.

These features are, nowadays, better predicted by models, than expressed by empirical calibrations.

The results summarized above have been obtained using, essentially, models with scaled-solar metal abundances. However, the entire problem of describing the clump behaviour with respect to age and metallicity gets even more complicated if we take into account that some stellar populations may be characterized by different initial metal distributions. We have demonstrated the sensitivity of the clump brightness to the metals relative abundances with our simulations of the Baade’s Window clump using α -enhanced evolutionary tracks. This adds a further variable – degree of α -enhancement – to the problem. Moreover, if the metal content Z is above solar – a situation that can be met even for $[\text{Fe}/\text{H}] = 0$ if α -enhancement is present – also the helium content Y becomes important in determining the absolute clump magnitude (see GGWS98). Therefore, in these cases a fourth variable is to be considered: the helium-to-metal enrichment ratio.

The correct approach to using the red clump as a distance indicator is therefore to evaluate the population corrections ΔM_I^{RC} – using population synthesis models – for

each individual object, provided that evaluations of the SFR and AMR do exist. In addition, informations on $[\alpha/\text{Fe}]$ and reasonable assumptions about the helium-to-metal enrichment ratio are needed. These occurrence, however, raises a fundamental question about the accuracy of the red clump as distance indicator. Udalski (1998b) emphasizes the advantages of the red clump with respect to other widely used standard candles such as Cepheid and RR Lyrae stars, these being mainly: (1) the existence of larger samples of red clump stars in galaxies with respect to Cepheids and RR Lyrae; (2) the very precise calibration of the absolute red clump brightness for the Solar Neighbourhood; (3) the existence of only a weak and empirically calibrated dependence of the red clump brightness on the metallicity. However, now that one has demonstrated that these empirical relations have no general validity, the red clump does not seem anymore to be a very reliable standard candle. At least, any determination of red clump distances requires the critical evaluation of the population effects, then implying that the red clump method cannot be meaningfully applied to objects for which there are no determinations of the SFR and AMR, *unless errors up to ≈ 0.3 mag are to be accepted.*

On the other hand, stellar evolution and population synthesis theory provide potentially important tools for the interpretation of clump data in nearby galaxies. We hope this paper has provided convincing examples of this.

ACKNOWLEDGMENTS

Thanks are due to S. Cassisi, M. Groenewegen, P. Marigo, and A. Weiss, for their useful comments and suggestions. We acknowledge the referee, B. Pagel, for the suggestions that improved the final presentation of this paper. X. Hernandez, M. Mollá, and H. Rocha-Pinto kindly provided us their results in computer-readable form. We gratefully acknowledge the hospitality of MPA during several visits.

REFERENCES

- Alonso A., Arribas S., Martínez-Roger C., 1996, A&AS 117, 227
 Barbuy B., 1999, ApSS 265, 319
 Bertelli G., Mateo M., Chiosi C., Bressan A., 1992, ApJ 388, 400
 Bertelli G., Nasi E., 2000, preprint.
 Bica E., Geisler D., Dottori H., Clariá J.J., Piatti A.E., Santos Jr. J.F.C., 1998, AJ 116, 723
 Carraro G., Chiosi C., 1994, A&A 287, 761
 Carraro G., 2000, in *The Chemical Evolution of the Milky Way: Stars versus Clusters*, eds. F. Matteucci, F. Giovanelli, in press.
 Carretta E., Gratton R., Clementini G., Fusi Pecci F., 2000, ApJ 533, 215
 Castellani V., Degl'Innocenti S., Girardi L., Marconi M., Prada Moroni P.G., Weiss A., 2000, A&A 354, 350
 Cayrel de Strobel G., Soubiran C., Friel E.D., Ralite N., François P., 1997, A&AS 124, 299
 Cole A.A., 1998, ApJ 500, L137
 Dolphin A., 2000, MNRAS 313, 281
 Dopita M.A., Vassiliadis E., Wood P.R., Meatheringham S.J., Harrington J.P., et al., 1997, ApJ 474, 188
 Elson R.W., Gilmore G.F., Santiago B.X., 1997, MNRAS 298, 157
 Feast M.W., Catchpole R.M., 1997, MNRAS 286, L1
 Feast M., 2000, PASP 111, 775
 Figer D.F., Kim S.S., Morris M., Serabyn E., Rich R.M., McLean I.S., ApJ 525, 750
 Frogel J.A., 1988, ARA&A 26, 51
 Frogel J.A., Tiede G.P., Kuchinski L.E., 1999, AJ 117, 2296
 Fuhrmann K., 1998, A&A 338, 161
 Geha M.C., Holtzman J.A., Mould J.R., et al., 1998, 115, 1045
 Girardi L., Bica E., 1993, A&A 274, 279
 Girardi L., 1999, MNRAS 308, 818
 Girardi L., 2000, in *The Chemical Evolution of the Milky Way: Stars versus Clusters*, eds. F. Matteucci, F. Giovanelli, in press (astro-ph/9912309).
 Girardi L., Groenewegen M.A.T., Weiss A., Salaris M., 1998, MNRAS 301, 149 (GGWS98)
 Girardi L., Bressan A., Bertelli G., Chiosi C., 2000, A&AS, 141, 371
 Gratton R., Fusi Pecci F., Carretta E., Clementini G., Corsi C.E., Lattanzi M., 1997, ApJ 491, 749
 Hatzidimitriou D., 1999, in *IAU Symp 190, New Views of the Magellanic Clouds*, p. 299
 Hernandez X., Gilmore G., Valls-Gabaud D., 2000a, MNRAS 317, 831
 Hernandez X., Valls-Gabaud D., Gilmore G., 2000b, MNRAS 316, 605
 Hill V., François P., Spite M., Primas F., Spite F., 2000, A&A, in press
 Høg E., Flynn C., 1998, MNRAS 294, 28
 Holtzman J.A., Light R.M., Baum W.A., Worthey G., Faber S.M., et al., 1993, AJ 106, 1826.
 Holtzman J.A., Mould J.R., Gallagher J.S., Watson A.M., Grillmair C.J., et al., 1997, AJ 113, 656
 Holtzman J.A., Gallagher J.S., Cole A.A., Mould J.R., Grillmair C.J., et al., 1999, AJ 118, 2262
 Hurley-Keller D., Mateo M., Nemej J., 1998, AJ 115, 1840
 Jimenez R., Flynn C., Kotoneva E., 1998, MNRAS 299, 515
 Kuhn J.R., Smith H.A., Awley S.L., 1996, ApJ 469, L93
 McWilliam A., 1990, ApJS 74, 1075
 McWilliam A., Rich R.M., 1994, ApJS 91, 749
 Mighell K.J., 1997, AJ 114, 1458
 Mollá M., Ferrini F., Gozzi G., 2000, MNRAS 316, 345
 Ng Y.K., Bertelli G., Chiosi C., Bressan A., 1996, A&A 310, 771
 Olsen K.A.G., 1999, AJ 117, 2244
 Olszewski E.W., Suntzeff N.B., Mateo M., 1996, ARA&A 34, 511
 Ortolani S., Renzini A., Gilmozzi R., Marconi G., Barbuy B., Bica E., Rich R.M., 1995, Nature 377, 701
 Paczyński B., 1998, Acta Astr. 48, 405
 Paczyński B., Stanek K.Z., 1998, ApJ 494, L219
 Paczyński B., Udalski A., Szymanski M., Kubiak M., Pietrzynski G., Soszynski I., Wozniak P., Zebrun K., 1999, Acta Astr. 49, 319
 Pagel B.E.J., Tautvaisiene G., 1998, MNRAS 299, 535
 Perryman M.A.C., et al., 1997, A&A 323, L49
 Piatti A.E., Geisler D., Bica E., Clariá J.J., Santos Jr. J.F.C., Sarajedini A., Dottori H., 1999, AJ 118, 2865
 Popowski P., 2000, ApJ 528, L9
 Reid M.J., 1993, ARA&A 31, 345
 Rich R.M., 1999, in *From Extrasolar Planets to Cosmology: The VLT Opening Symposium*, ESO Astroph. Symp., eds. J. Bergeron & A. Renzini Springer-Verlag, p. 275.
 Rocha-Pinto H.J., Maciel W.J., Scalo J., Flynn C., 2000a, A&A 358, 850
 Rocha-Pinto H.J., Scalo J., Maciel W.J., Flynn C., 2000b, A&A 358, 869
 Romaniello M., Salaris M., Cassisi S., Panagia N. 2000, ApJ 530, 738
 Salaris M., Weiss A., 1998, A&A 335, 943
 Salasnich B., Girardi L., Weiss A., Chiosi C., 2000, A&A in press

- Sarajedini A., 1999, *AJ* 118, 2321
- Schuster W.J., Nissen P.E. 1989, *A&A* 221, 65
- Smecker-Hane T., Stetson P.B., Hesser J.E., Vandenberg D.A., 1996, in *ASP Conf. Ser. 98, From Stars to Galaxies*, ed. C. Leitherer, U. Fritze-von Alvensleben and J. Huchra, (ASP: San Francisco), p. 328
- Stanek K.Z., Garnavich P.M., 1998, *ApJ* 503, L131
- Stanek K.Z., Zaritsky D., Harris J., 1998, *ApJ* 500, L141
- Stappers B.W.; Mould J.R., Sebo K.M., Holtzman J.A., Gallagher J.S., et al., 1997, *PASP* 109, 292
- Tinsley B.M., 1980, *Fund. Cosm. Physics* 5, 287
- Twarog B.A., Anthony-Twarog B.J., Bricker A.R. 1999, *AJ* 117, 1816
- Udalski A., Szymański M., Kubiak M., Pietrzyński G., Woźniak P., Żebruń K, 1998, *Acta Astr.* 48, 1
- Udalski A., Szymański M., Kubiak M., Pietrzyński G., Soszyński I., Woźniak P., Żebruń K, 1999, *Acta Astr.* 49, 201
- Udalski A., 1998a, *Acta Astr.* 48, 113
- Udalski A., 1998b, *Acta Astr.* 48, 383
- Udalski A., 2000, *ApJ* 531, L25
- Vallenari A., Chiosi C., Bertelli G., Aparicio A., Ortolani S., 1996, *A&A* 309, 367
- Westerlund B.E., 1997, *The Magellanic Clouds*, Cambridge University Press.
- Zaritsky D., 1999, *AJ* 118, 2824